5-2019

The effect of cysteine-reactive catechol antioxidants on alcohol dehydrogenase as a model for oxidative stress in neurodegenerative disease

Rachel Smith

The effect of cysteine-reactive catechol antioxidants on alcohol dehydrogenase as a model for oxidative stress in neurodegenerative disease

A thesis submitted in partial fulfillment of the requirement for the degree of Bachelor in Science in Neuroscience from the College of William and Mary

By

Rachel Smith

Accepted for _____

_____
Dr. Lisa Landino, Advisor

_____
Dr. Randolph Coleman

_____
Dr. M. Christine Porter

TABLE OF CONTENTS

ABSTRACT

The cellular mechanisms underlying age-related neurodegeneration, especially in disease states, are poorly understood. Oxidative stress has been heavily implicated as one factor both produced by and contributing to the progression of neurodegenerative diseases such as Alzheimer's disease. In particular, it can destroy a cell's ability to produce energy through aerobic and anaerobic respiration, thus leading to the death of individual cells and brain tissues as a whole. This study focuses on the relationship between oxidative stress and energy production in disease states. In particular, we examine the ability of catechol molecules to take on pro-oxidative properties and modify the enzyme alcohol dehydrogenase (ADH), both *in vitro* and in a yeast cellular model. Using enzyme kinetic assays, we found that when oxidized, certain catechols are able to inhibit isolated ADH activity. Though this result was not clearly replicated *in vivo* in yeast cellular models, we speculate that this is due to the complexity and adaptive abilities of a living system. Furthermore, native gel electrophoresis demonstrated that treatment with catechols does not induce detectable conformational change in ADH. These results suggest that oxidized catechols are able to inhibit ADH activity, but living cells may be able to adapt to the presence of these exogenous molecules through alteration of gene and protein expression. Further studies utilizing yeast cell lysis and fluorescence techniques are required to definitively ascertain antioxidant molecules' effects on the proteins in living cells. These results have implications for the role of oxidative stress in age-related neurodegenerative disease in relation to impact on energy production.

INTRODUCTION

Age-related and neurodegenerative diseases, namely Alzheimer's disease (AD), are almost as poorly understood as they are widespread. Several specific cellular mechanisms have been proposed for the pathogenesis of AD, but these explanations are non-comprehensive and fallible. Thus, it is of critical importance to further examine these molecular pathways and all aspects related to them in order to obtain a holistic understanding for treatment and prevention purposes.

Oxidative stress is one process that has been heavily implicated in the development and progression of degenerative disease. It involves the production and proliferation of highly reactive free radicals which damage essential cellular components, including proteins and lipids. When important cellular structures are undermined, the cell itself may die, ultimately leading to the widespread death of brain tissue (and thus functional loss). Oxidative stress becomes particularly important in the context of energy production. Energy production through glycolysis, the Citric Acid Cycle, and oxidative phosphorylation is arguably the most important function a cell performs. If any stage of this process is compromised, the cell itself is weakened, and in extreme cases, dies. Thus, oxidative stress damaging any element of cellular energy production, whether it be a glycolytic enzyme or the mitochondria itself, can cause the cell to deteriorate and possibly die.

This study focuses on this intersection of oxidative stress and energy production in a disease topic. Specifically, we investigate the role of antioxidants in oxidative stress and neurodegenerative disease. Antioxidants are typically heralded by mass media as miracle molecules that can protect the brain from cognitive decline. However, recent scientific literature suggests that these molecules, though physiologically essential, are only beneficial in moderation

and can in fact have pro-oxidative effects that further progress damage. We explore the impact of a specific category of antioxidant molecules, oxidized catechols, on the structure and function of the glycolytic enzyme alcohol dehydrogenase (ADH) in a yeast cellular model. When then cell cannot rely on mitochondrial respiration, ADH is upregulated in order to produce more ATP through a process known as the Warburg effect. Thus, its functional ability is of clear critical importance in disease states.

The goal of this study is to examine the pro-oxidative potential of catechol antioxidant molecules in the context of ADH structure and function. Based on previous studies, we hypothesize that when oxidized (as would be physiologically relevant in disease states with oxidative stress), these molecules can produce counterproductive effects and actually undermine the functional abilities of ADH. We investigate this relationship in the following capacities: 1. The ability of oxidized catechols (ortho-quinones) to inhibit isolated ADH *in vitro*, 2. The ability of ortho-quinones to enter yeast cells that have been given 'food' to produce ethanol and inhibit ADH *in vivo*, and 3. The ability of ortho-quinones to structurally modify ADH and induce conformational change. These results can be compared to similar work done in the lab regarding the mammalian equivalent of ADH, lactate dehydrogenase (LDH).

Cognitive decline and general neurodegeneration are poorly understood mechanistically, especially in disease states. This renders the development of effective treatment and prevention methods very difficult, as it is impossible to account for all components of a molecular mechanism that is not comprehensively understood. The results of this experiment implicate just one of many potential pathological pathways in AD and general age-related decline, showing how an important glycolytic enzyme in a cellular model responds in AD conditions of oxidative stress. This study is of particular relevance to the general population, as it implicates the role of

generally revered antioxidants in actually enhancing the effects of oxidative stress in disease states.

BACKGROUND

Alzheimer's Disease

Alzheimer's disease (AD) is the most common form of dementia, accounting for about 70% of cases worldwide. It is a progressive neurodegenerative disorder characterized by nerve cell atrophy and widespread neuronal loss, primarily affecting regions including the hippocampus, entorhinal cortex, amygdala, neocortex, and some subcortical areas. (Revett, Baker, Jhamandas, & Kar, 2013).

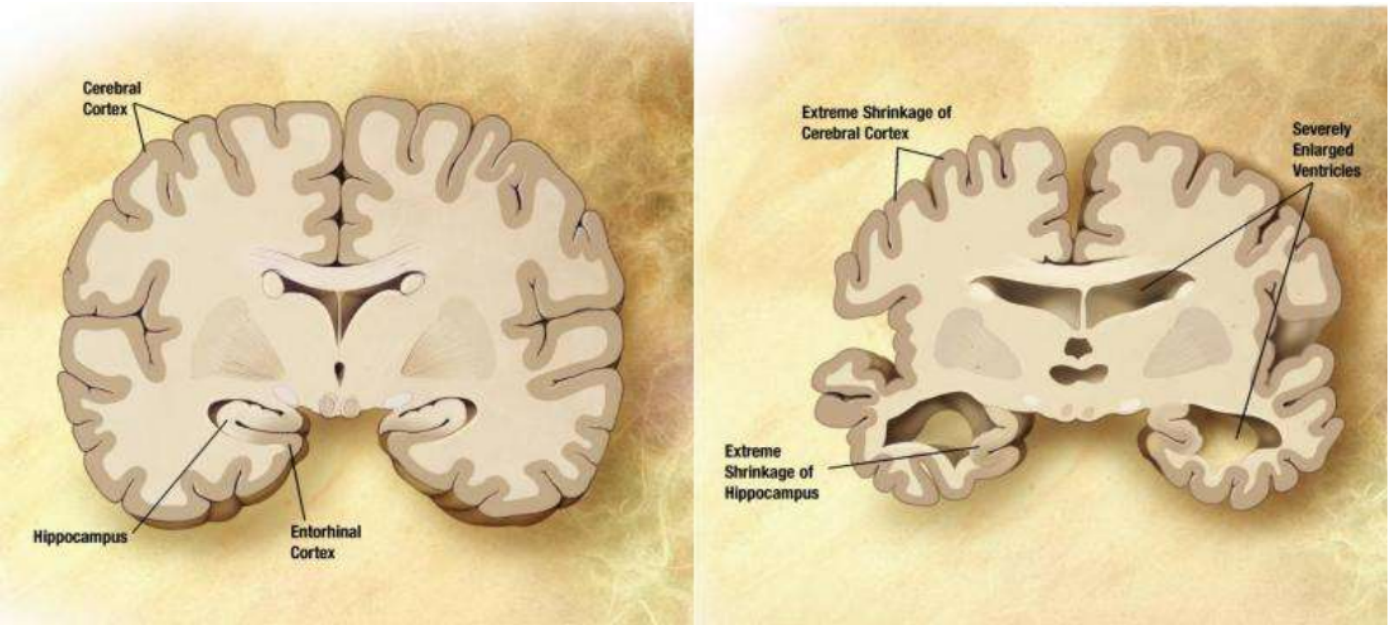

Figure 1: Alzheimer's disease is associated with physical neuronal loss in major brain areas involved in cognition and emotion. Gaping holes such as those depicted are seen in the brains of Alzheimer's patients post-mortem.

Image taken from: Institute for Basic Science

The effects of this degeneration are clinically observed through a variety of associated symptoms including cognitive impairment and memory loss, loss of language and motor skills, and changes in behavior such as confusion and paranoia (Huang & Jiang, 2009). Physiologically,

AD is characterized by two structural neuropathologies – senile or neuritic plaques and neurofibrillary tangles (NFTs).

The Amyloid Hypothesis & APP processing

The amyloid hypothesis has been the dominant explanation for the pathogenesis of AD for almost three decades. It states that the accumulation and deposition of amyloid β (Aβ) peptides into amyloid plaques is the primary cause of AD pathogenesis (Hardy & Selkoe, 2002). In order to fully understand the pathological deposition of these plaques, it is critical to understand their origins and the dysfunctions that lead to their formation.

APP processing

Aβ peptides are derived from cleavage of amyloid precursor protein, or APP. Once synthesized in the soma, APP is transported through the axon to the terminal of a neuron, where it is cleaved by three major proteases – α-secretase, β-secretase and the γ-secretase complex. Cleavage is initiated by α-secretase which divides the APP into two pieces. One of these fragments is then passed onto the β-secretase, which cleaves the fragment into further pieces. Finally, the multiprotein γ-secretase complex cleaves one of these fragments, thus releasing APP intracellular domain (AICD) as well as Aβ in the extracellular space of the synaptic terminal (Figure 2). In normal physiological processing, these small Aβ fragments are rapidly degraded and removed (Chow et al., 2010; Kamentani & Hasegawa, 2018).

Aβ peptide production

This mechanism describes non-pathological cleavage by these proteases; however, mutations in APP or the proteases can cause improper cleavage of APP resulting in the pathological accumulation of Aβ peptides, which serves as the basis of the amyloid hypothesis. These mutations tend to favor β- and γ-secretase over α-secretase, resulting in 40-42 amino acid

chains to be released, as opposed to the physiologically normal 26 (Hardy & Selkoe, 2002). These abnormally long peptide sequences are unable to be degraded as is physiologically standard, and instead aggregate into β-sheets to ultimately form extracellular senile plaques (Revett et al., 2013)(Figure 2).

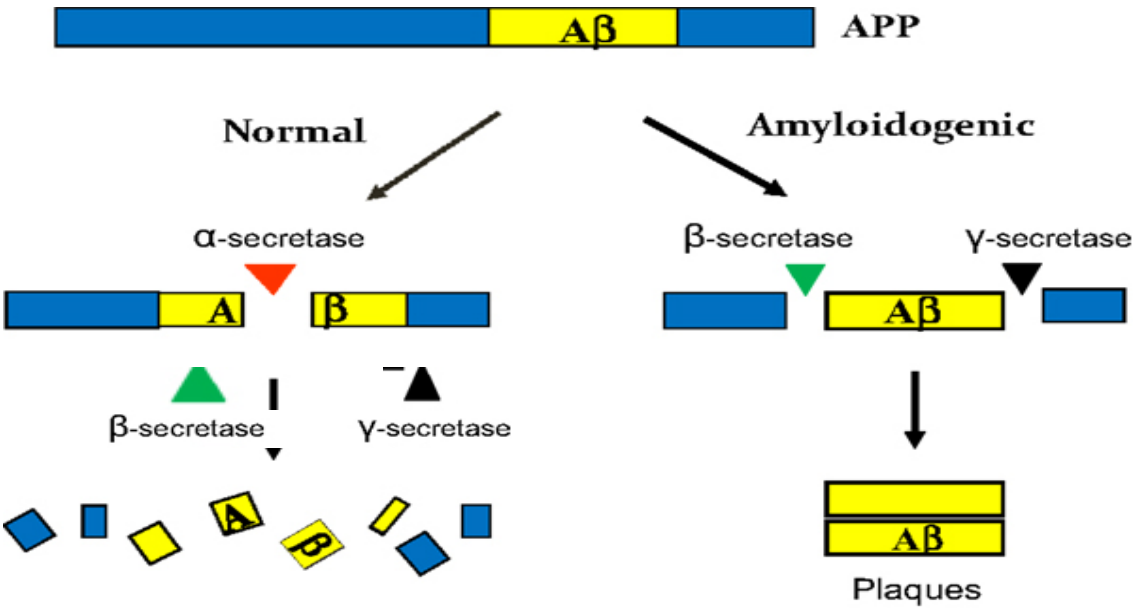

Figure 2: Non-pathological APP processing (left pathway) involves cleavage first by α-secretase, then β-secretase and γ-secretase break the fragments into smaller pieces. Pathological mutations in the secretases leading to β- and γ-secretase overactivity or α-secretase underactivity result in the creation of Aβ peptides that are too big for the cell to process normally (right pathway). These peptides then accumulate into toxic amyloid plaques.

Figure taken from: Chen, M. (2015). The maze of APP processing in Alzheimer's disease: where did we go wrong in reasoning? *Frontiers in Cellular Neuroscience*. doi: 10.3389/fncel.2015.00186

Several different mutations in the proteases and APP itself have been implicated in this improper cleavage. For one, an increase in β-secretase activity is associated with an elevation in the level of Aβ peptides, and higher concentrations of this protease in certain regions of the brain are documented in some cases of sporadic AD. These activity-enhancing mutations are especially prominent in situations involving cellular stress, such as hypoxia, ischemia, energy deprivation, and oxidative stress. In contrast, a complete ablation of β-secretase expression prevents any amyloid plaques from accumulating in mouse models. This indicates that an

increase in activity in β-secretase is pathological, presumably because it cleaves the APP before α-secretase can, therefore skipping one cleavage step and resulting in a longer peptide chain. With regard to γ-secretase, several studies have found that knocking out various proteins within the complex reduce and can even reverse amyloid pathology and its associated cognitive deficits (Chow et al., 2010). On the other hand, studies have shown that enhancing α-secretase activity can decrease Aβ production and plaque deposition, correlated with a reduction in cognitive deficits. Based on these results, mutations that enhance β- and γ-secretase activity or reduce α-secretase activity lead to the improper cleavage of APP and the release of abnormally long Aβ peptide chains into the extracellular space. These fragments are unable to be degraded and instead aggregate into amyloid plaques. These plaques are then associated with neuronal loss in the entorhinal cortex, hippocampus, and associated cortices (Revett et al., 2013). Thus, the amyloid hypothesis claims that the formation of these plaques due to improper APP processing or the failure to remove extracellular Aβ is the primary event in AD pathogenesis (Hardy & Selkoe, 2002).

Role of Neurofibrillary Tangles

The other neuropathological hallmark associated with AD comes in the form of neurofibrillary tangles, or NFTs. These abnormal structures are composed of tau proteins which have assembled into β-pleated sheets and then aggregated into paired helical filaments (PHF) (Zhou et al., 2018). Tau is a positively charged microtubule-associated protein, meaning it interacts with the negatively charged tubulin (microtubule monomers) to allow for microtubule assembly and stability (Kametani & Hasegawa, 2018). The binding of tau to microtubules is regulated by post-translational modifications including phosphorylation, glycosylation, and ubiquitination. However, if tau is hyperphosphorylated due to mutations in the protein

machinery, it loses its positive charge and is unable to bind the negatively charged tubulin. It then begins to polymerize, forming PHFs (Revett et al., 2013) (Figure 3). Without tau to stabilize it, the microtubule cannot polymerize to perform its transportation and structural functions. As a result, the neuron dies, and NFTs are left behind in its stead.

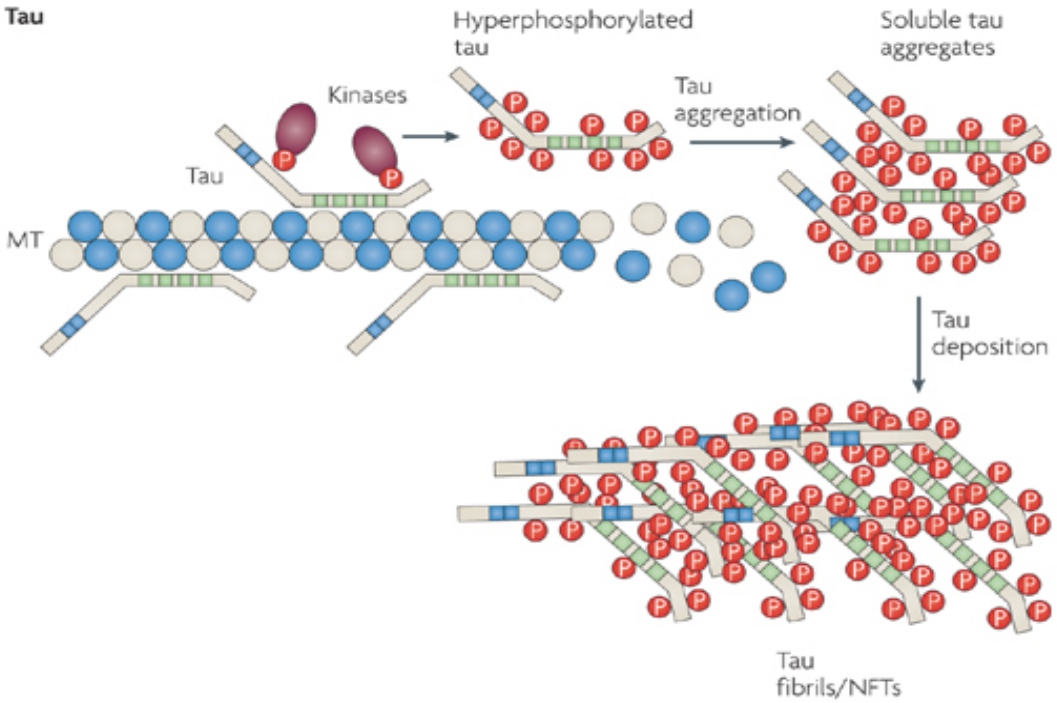

Figure 3: Dysregulation of kinases leads to hyperphosphorylation and aggregation of tau into NFTs. As a result, the microtubule becomes unstable and breaks apart, ultimately resulting in neuronal death.

Image taken from: Neuroscience Fundamentals

Beyond hyperphosphorylation, proteolysis of tau is also heavily implicated in AD. Research has found truncation of tau at Asp421 by caspase 3 may initiate the formation of PHF at early stages of the disease (Zhou et al., 2018). Both hyperphosphorylation and proteolysis of tau lead to the aggregation of tau into tangles and neuronal death associated with AD.

Reactive Oxygen Species and Oxidative Stress

Scientists hypothesize that one of the methods by which Aβ plaques induce neurotoxicity is by facilitating oxidative stress; therefore, this has been a target of recent research seeking to

elucidate the underlying mechanism, or pathogenesis, of AD. On a molecular level, oxidative stress begins with the formation of free radicals in a biological system. Free radicals are uncharged molecules with unpaired valence electrons. They are highly unstable and will react with any available source in order to form an electron pair and increase stability (Lu, Lin, Yao, & Chen, 2010). (If the free radical involves an oxygen atom, it is termed 'reactive oxygen species' (ROS) and the terms are often used interchangeably.) ROS are physiologically normal phenomena that are formed naturally in a biological system during cellular activities, such as mitochondrial metabolism, and can have physiologically beneficial functions (Carocho & Ferreira, 2013). In addition to natural production, free radicals can also be derived from external sources and environmental stressors that the organism is exposed to, including cigarette smoke, x-rays, pollutants, and even exercise.

'Oxidative stress' is the process in which free radicals damage a biological system by seeking to stabilize themselves via reactions with important substrates, including physiologically essential proteins, lipids, and DNA. This can disrupt information flow and signaling in individual cells and eventually cascade into the death of entire neuronal networks (Lobo, Patil, Phatak, & Chandra, 2010). Oxidative stress has been heavily implicated in neurodegenerative diseases including AD, as both Aβ and NFT are reportedly major sources of ROS, and these free radicals can then in turn cause further damage to biological substrates (Smith, Rottkamp, Nunomura, Raina, & Perry, 2000).

Role of Antioxidants

Antioxidants scavenge ROS

With the increasing amount of research indicting the role of oxidative stress in neurodegenerative disease, much attention has been turned to the role of antioxidants as a

mechanism to counteract the devastating effects of free radicals. Antioxidants are defined by Halliwell (2007) as "any substance that delays, prevents or removes oxidative damage to a target molecule" (p. 1147). These substances serve as a defense system against oxidative stress primarily by accepting or donating an electron to the free radical and stabilizing it, thereby removing its ability to react with physiologically important substrates. Due to its chemical structure, the antioxidant is theoretically able to remain stable and unreactive despite having an unpaired electron itself, thus curing the biological system of the risk of oxidative damage (Lobo et al., 2010).

Antioxidants are found both endogenously in cells and as exogenous molecular compounds from food. Endogenous antioxidants include enzymes such as catalase and the glutathione systems, as well as melatonin (Lobo et al., 2010). However, this built-in antioxidant system is insufficient to properly balance out free radical concentrations, thus it is essential that humans acquire additional antioxidants through their diet to protect their cells (Carocho & Ferreira, 2013). Ultimately, the endogenous and exogenous antioxidant systems interact to check the scavenging prowess of free radicals. Exogenous antioxidants are found primarily in plant-based compounds including fruits, vegetables, grains, spices, and herbs. These plant extracts contain several different categories of antioxidant molecules, including phenols, flavonoids, and carotenoids (Bouayed & Bohn, 2010). Since these exogenous antioxidants are necessary to supplement the endogenous systems, it is known that nutrition plays a crucial role in the prevention of many different diseases rooted in oxidative stress (Lobo et al., 2010).

Phenolic antioxidants

Phenols, a class of exogenous, plant-based antioxidants, are molecules composed of a benzene ring with a hydroxyl group attached. They are able to scavenge ROS and maintain

stability due to their aromaticity, thereby preventing damage to the cell. In catechols, a subset of phenols, two hydroxyl groups are attached to the benzene ring. This study focuses on ortho-phenols, meaning the hydroxyl groups are attached to adjacent carbons. Catechol-based compounds include any molecule with this basic structure as a backbone, and other substituents attached (Bolton & Dunlap, 2017). Examples include caffeic acid and the neurotransmitter dopamine (Figure 4).

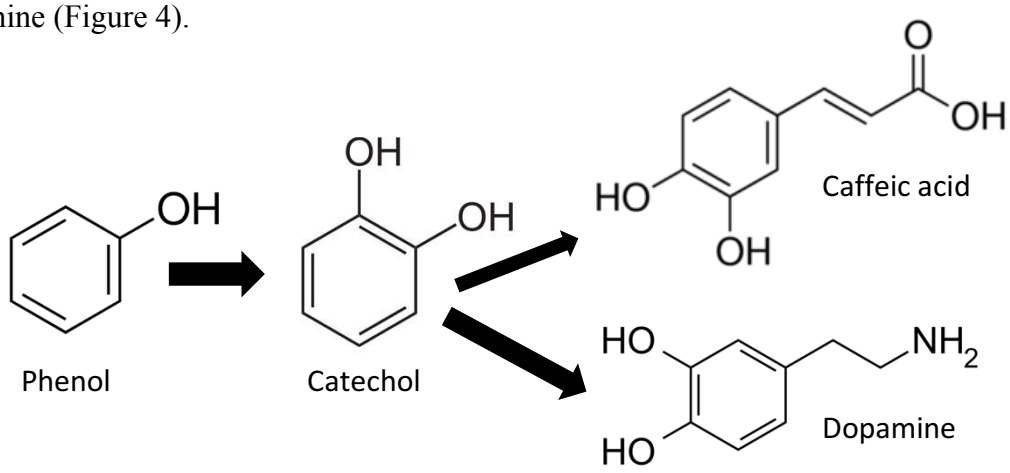

Figure 4: Antioxidant compounds such as caffeic acid and dopamine are derived from phenols.

Structures taken from: Sigma-Aldrich

Catechols can be oxidized to o-quinones when scavenging free radicals. The oxidized structure includes two adjacent ketones and only two pi-bonds remaining in the aromatic ring (Figure 5).

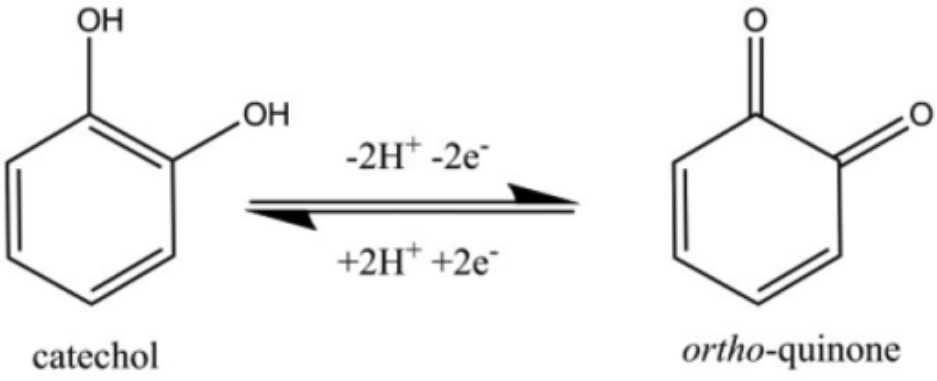

Figure 5: Oxidation of a catechol results in the formation of an ortho-quinone.

Image taken from: National Institutes of Health

This oxidation renders the alpha-carbon highly electrophilic and prone to reaction with a nucleophile. In biological systems, thiol groups, including cysteine residues in proteins, serve as ubiquitous nucleophiles. Thiols can undergo a Michael addition with the oxidized quinone, in which the sulfur atom forms a bond with the alpha-carbon and the quinone is reduced back to a catechol (Figure 6).

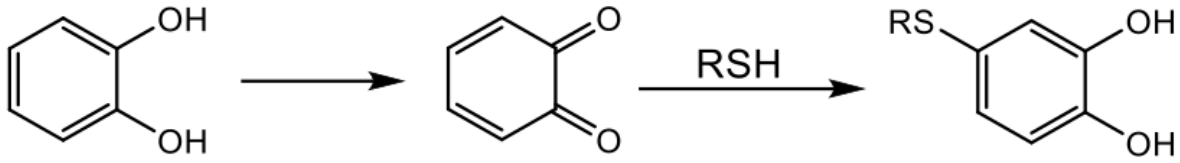

Figure 6: A basic Michael addition. The first step includes oxidation of the catechol, while the step is a nucleophilic attack of the thiol. Oxidized catechols readily react with available thiol groups (in this case, a cysteine) serving as the nucleophile. This reaction disrupts the structure of the protein as the cysteine is now covalently bound to an external molecule.

Potential pro-oxidative effects of antioxidants

The ability of antioxidants to react with cysteine residues demonstrates their pro-oxidative potential to damage proteins structurally and functionally. Prooxidants are molecules that induce oxidative stress by forming reactive species or inhibiting antioxidants (Carocho & Ferreira, 2013). Recent research has shown that most dietary antioxidants can have prooxidant behavior, depending highly on their concentration and neighboring molecules (namely metal ions). As was previously described, maintaining the balance between free radicals and antioxidants is critical, meaning high doses or concentrations of antioxidants will disrupt this balance and cause cellular toxicity through several different methods. When antioxidants react with free radicals, they become radicals themselves. If they are unable to adequately stabilize the electron, they, too, will be reactive and potentially damaging (Bouayed & Bohn, 2010). Furthermore, antioxidants can serve as an intermediate in a process known as redox cycling, in which they pass on the electron to another cellular substrate, thus serving a catalytic role.

Additionally, catechol compounds can become oxidized under conditions of oxidative stress, and are subsequently prone to react with nucleophilic cysteines (Figure 6). This damages the protein in the same way that the free radical would have had the antioxidant not been present in the first place. Thus, antioxidants have the potential to induce oxidative stress under certain conditions.

Glycolysis and Glycolytic Enzymes

Glycolysis in physiologically stable cells

Glycolysis is a ten-step process occurring in the cytosol that converts glucose to pyruvate, producing two net ATP molecules per unit glucose as a result. In conditions with normal oxygen levels, pyruvate is then shuttled through the citric acid cycle in the mitochondrial matrix to generate reduced electron carriers NADH and $FADH_2$. These electron carriers travel through the electron transport chain in the mitochondria to produce a total of 32 molecules of ATP using oxidative phosphorylation (Figure 7). Oxidative phosphorylation requires oxygen to occur, and it produces many more molecules of ATP per unit glucose than does glycolysis alone.

In hypoxic conditions, however, pyruvate is unable to be sent to the mitochondria to complete the metabolic process, as oxygen levels are inadequate for oxidative phosphorylation. Instead, pyruvate remains in the cytosol, where it is converted into lactate using the enzyme lactate dehydrogenase (LDH) (Figure 7). This process, known as anaerobic respiration or anaerobic glycolysis, generates more NAD+, which is then used to enhance glycolysis rates and increase ATP production (Figure 8). Using this pathway, the cell facilitates increased energy production to compensate for its inability to undergo oxidative phosphorylation (Kim & Dang, 2005). In plant and yeast cells, alcohol dehydrogenase (ADH) serves as the LDH correlate, and converts acetaldehyde (derived from pyruvate) into ethanol to produce NAD+ and increase ATP production in hypoxic conditions.

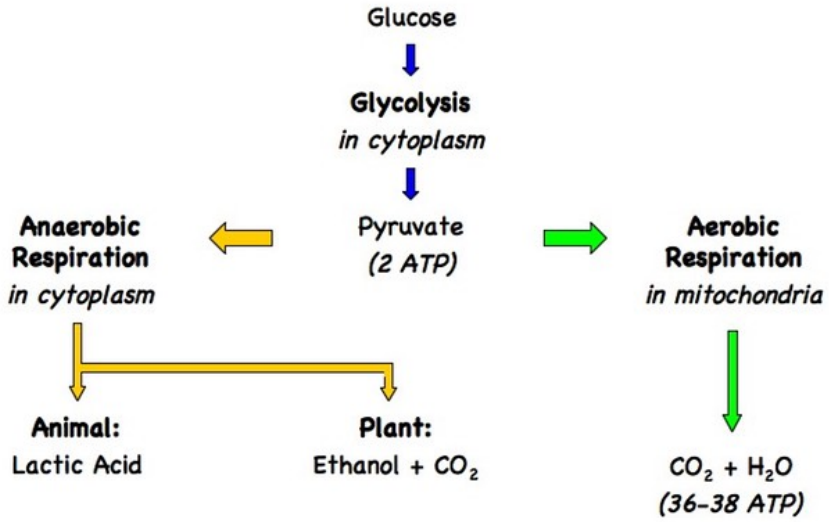

Figure 7: Under normal oxygen levels, cells undergo both glycolysis and aerobic respiration to produce maximal amounts of ATP. However, under hypoxic conditions, the cell undergoes anaerobic respiration because it is unable to complete oxidative phosphorylation.

Image taken from: BioNinja

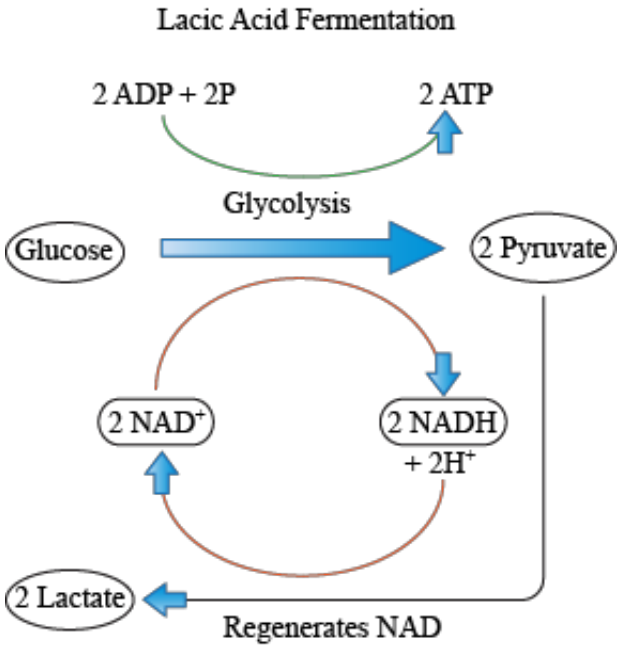

Figure 8: Anaerobic respiration facilitates increased energy production as it creates NAD+ to be used in glycolysis. Though glycolysis only produces 2 ATP per unit glucose (as opposed to the 32 produced using aerobic respiration), it becomes the only source of energy under hypoxic conditions and therefore must be utilized.

Image taken from: wvu.edu

Despite extra efforts to increase ATP output using just anaerobic respiration, there is still not nearly enough energy produced without oxidative phosphorylation. Therefore, cells also respond to insufficient oxygen levels by upregulating the expression of genes for glycolytic

enzymes (Kim & Dang, 2005). In doing so, the cell increases the rate of energy production via glycolysis as a temporary solution to ATP deficits in hypoxic conditions.

Glycolysis in disease states

In disease states involving oxidative stress, such as AD, free radicals target and damage the mitochondria. Similar to hypoxic conditions observed in healthy cells, oxidative stress thus inhibits the cell's ability to undergo complete mitochondrial respiration. As such, diseased cells tend to upregulate glycolysis to increase ATP production without oxidative phosphorylation. Even with sufficient oxygen, diseased cells increase lactate (or ethanol, in the case of yeast) production because oxygen levels become irrelevant without a functioning mitochondria to facilitate the reactions. This observation is known as the Warburg effect, and indicates the cell is undergoing anaerobic respiration in an effort to produce more ATP despite a malfunctioning mitochondria. The upregulation of anaerobic glycolysis has been detected in AD cells, thus implicating the importance of glycolytic enzymes in disease pathology (Kim & Dang, 2005).

Alcohol Dehydrogenase

Alcohol dehydrogenase (ADH) is an enzyme under the umbrella class of enzymes called NAD-dependent oxidoreductases, which catalyze the reversible oxidation of primary and secondary alcohols to aldehydes and ketones (Raj, Ramaswamy, & Plapp, 2014). During anaerobic respiration, ADH reduces acetaldehyde (derived from pyruvate) to form ethanol, the end product of yeast fermentation (Figure 9). In doing so, NADH is oxidized back to NAD+ to be used in glycolysis for ATP production in hypoxic conditions.

Though it is a topic of semantic contention, ADH will be referred to as a glycolytic enzyme for the purposes of this paper. Technically, glycolysis consists only of ten enzyme-catalyzed steps to produce pyruvate. Only some consider ADH-catalyzed ethanol fermentation

(or the mammalian equivalent: LDH-catalyzed lactic acid fermentation) as the "eleventh step" of glycolysis, as it is not essential to the process itself. However, this study looks at ADH in the context of energy production in disease states, thus it is considered a glycolytic enzyme.

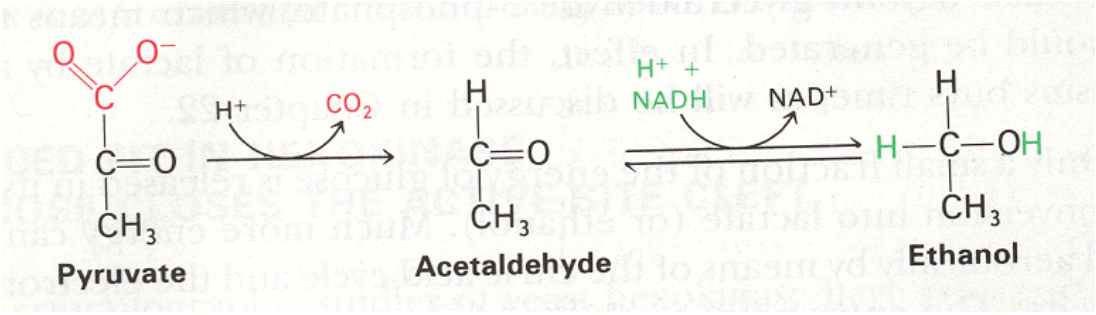

Figure 9: Alcohol dehydrogenase converts acetaldehyde to ethanol during anaerobic respiration in yeast, thereby regenerating NAD+.

Image taken from: chem.uwec.edu

Yeast (*Saccharomyces cerevisiae*) ADH is a homotetramer, with each subunit composed of 347 amino acid residues.

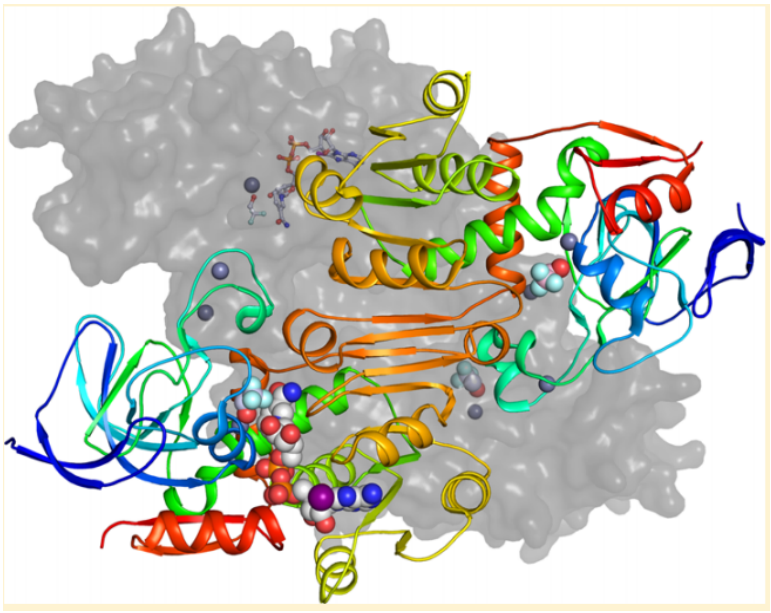

Figure 10: Yeast ADH structure

Image taken from: Raj, Ramaswamy, & Plapp,

Each unit contains four different subunits arranged with similar dimers, named AB and CD (Figure 10). The A and C subunits are structurally similar with a bound coenzyme in closed

conformation. The catalytic site includes a zinc in classic coordination with Cys-43, Cys-153, and His-66. Subunits B and D, on the other hand, have an open conformation, no bound enzyme, and a catalytic zinc in an alternative coordination with the same three amino acid residues as well as Glu-67. The catalytic zinc atoms are used to hold and position the hydroxyl group. They are chelated at the active site by the two cysteines, and chemical modifications of these residues are associated with loss of enzyme activity, as such modifications would disrupt the binding of substrates (Figure 12). Furthermore, intradimer interactions include a disulfide bond between the Cys-277 residues, and experiments disrupting this bond resulted in decreased enzyme stability and activity (Raj et al., 2014). Key cysteines are vulnerable targets under oxidative stress, as they are readily oxidized into disulfides and can also act as a nucleophile in reactions such as a Michael addition (Figure 6). Damaging cysteine residues alters critical aspects of the protein structure, thus theoretically compromising its function.

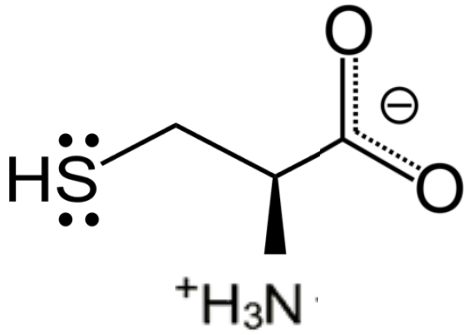

Figure 11: The structure of the amino acid cysteine. The functional group includes a sulfur atom with lone pair electrons that are highly nucleophilic. It is a hydrophobic, uncharged amino acid. The pKa of the carboxyl group is 1.96, while the pKa of the ammonium group is 8.18.

Image modified from: Wikipedia

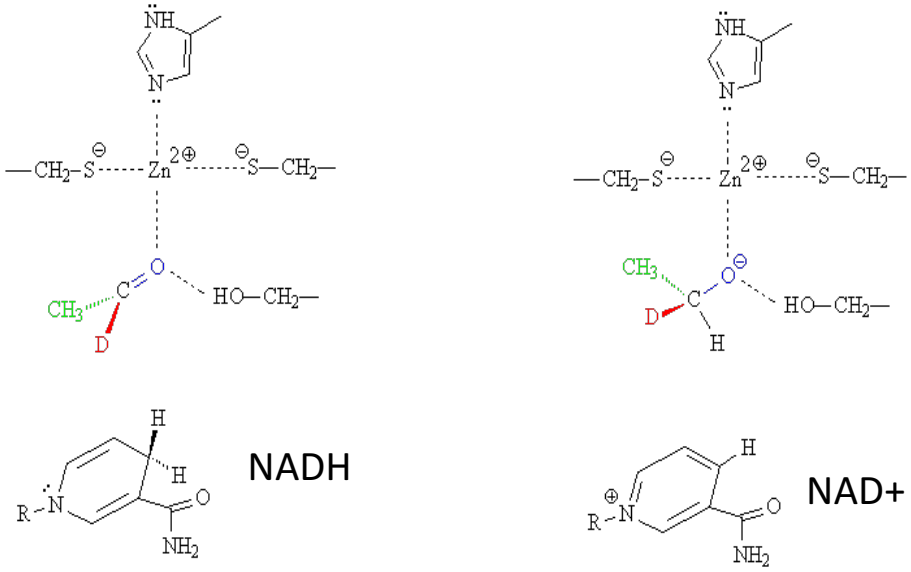

Figure 12: ADH active site includes a histidine and two cysteine residues to hold the catalytic zinc in place. Zinc is then able to position the hydroxyl group for oxidation by NADH. Without proper cysteine positioning, the protein would be unable to convert ethanol to acetaldehyde or vice versa.

Image taken from: mason.gmu.edu

In yeast, ADH serves to produce ethanol through fermentation. Human ADH, however, only catalyzes the reverse reaction, converting ethanol to acetaldehyde as a defense mechanism against the toxic molecule which can permanently damage the nervous system. This demonstrates the reversibility of the reduction reaction. Because of ADH's important role in anaerobic fermentation in hypoxic conditions and disease states, studying its activity in oxidative stress conditions is imperative in furthering understanding of these disease mechanisms.

Yeast as Cellular Model for Oxidative Stress

Yeast as a model organism

This study observes the effects of antioxidant-mediated oxidative stress on ADH in yeast as opposed to in the mammalian analogue LDH. The primary reason for using yeast instead of mammalian cells is that the former are generally much easier to work with and manipulate as they are far simpler eukaryotic organisms, but the essential cellular processes are conserved in yeast and humans. In the mid-1990s, yeast *Saccharomyces cerevisiae* became the first eukaryotic organism with a complete DNA sequence of its genome, as a result of a major research project

driven by the argument that yeast would serve as a model organism to facilitate the understanding of human DNA sequences. Like humans, yeast cells have a nucleus containing DNA packaged into chromosomes. There are genes in yeast and mammals that encode similar proteins, such as proteins of molecular systems (including ribosomes and cytoskeletons) and proto-oncogenes. Thus, comparisons can be made between the mammalian genome and the more fully understood yeast genome to hypothesize function of unknown mammalian genes (Botstein, Chervitz, & Cherry, 1997).

Most cellular and metabolic pathways known to occur in humans can be studied in yeast. For instance, much research regarding brain and nervous system development has been conducted using signaling proteins in yeast. Furthermore, yeast is particularly useful as a model system for disease states, including neurodegenerative diseases such as AD. Disease genes can be mapped by inheritance, cloned, and sequenced. This allows for the ethical manipulation of disease genotypes and subsequent observation of their cellular phenotypes. For example, yeast cells engineered to produce excessive amounts of pathological protein aggregates associated with Parkinson's disease show signs of damage and slow their growth patterns. Using these methodologies, researchers have demonstrated than many human diseases are the result of disruptions of basic molecular pathways such as DNA repair and cell division (Botstein et al., 1997). Thus, studying yeast can facilitate understanding of basic molecular processes in humans, and manipulating and interpreting yeast metabolic pathways can map directly onto mammalian analogies.

Yeast strains and ethanol production

Yeast can ferment ethanol from simple sugars in anaerobic conditions. *S. cerevisiae* have been used for thousands of years for alcohol production, as it gives high ethanol yield and can

withstand varying conditions, including a wide range of pH levels and temperatures (Azhar et al., 2017). When provided with 'food' (i.e. carbon sources) such as dried malt extract, yeast metabolize to produce ethanol, with the final conversion of acetaldehyde to ethanol being mediated by endogenous ADH. This experiment studies ADH activity in two different *S. cerevisiae*-based yeast strains – SafAle 05 and Belgian Strong Ale 565 (BS 565). The primary difference between the two strains is the incorporation of different additives, namely emulsifiers. BS 565 is able to produce more ethanol using the same carbon sources as SafAle 05.

Transport of phenolic antioxidant molecules into yeast cells

The focus of this study is on the ability of catechol-based antioxidant molecules to exhibit pro-oxidative effects by affecting yeast ADH activity. The *in vivo* experiments thus required the transport of these molecules into the yeast cells during growth and ethanol production periods, so that the antioxidants could potentially modify endogenous ADH. Due to their benzene ring, phenols are lipophilic molecules that can readily diffuse across membranes, following the concentration gradient (Sawada, Williams, Lutzke, & Raub, 1999). Thus, the catechol-based molecules used in this experiment were able to access yeast ADH without any additional enablement. In a larger context, antioxidants are also able to cross the blood brain barrier, and thus have easy access to exert their effects on neurons.

MATERIALS AND PROCEDURES

Materials

Proteins and cellular extracts

Yeast alcohol dehydrogenase (146,800 g/mol) and mushroom tyrosinase were obtained from Sigma-Aldrich. The SafAle 05 yeast strain was bought from Amazon, while the Belgian Strong 565 yeast strain was obtained from White Labs. The yeast cell cultures were then grown in lab by Dr. Lisa Landino.

Compounds

Nicotinamide adenine dinucleotide (NAD+), nicotinamide adenine dinucleotide + hydrogen (NADH), alcohol dehydrogenase (ADH), catechol, EGCG, and PP60 tea extract were obtained from Sigma-Aldrich. Caffeic acid, thiazolyl blue tetrazolium bromide (MTT), and phenazine methosulfate (PMS) were purchased from Acros Organics. Nitro blue tetrazolium chloride (NBT) and agarose were both obtained from Thermo Fisher Scientific. Hydrocaffeic acid was purchased from Alfa Aesar, 200 proof ethanol (EtOH) from Pharmco-Aaper, and Malt Extract Powder from HiMedia Laboratories. Acetaldehyde was purchased from Acros/Fisher.

Tea samples were extracted in boiling water from Trader Joe's Organic Green Tea, Yogi Green Tea Kombucha, Clipper Rise & Shine, and Guayaki Yerba Mate Organic. Hops samples were extracted in boiling water from YCHHOPS German Hallertau hops pellets, YCHHOPS United States Cascade hops pellets, and LD Carlson's Apollo hops pellets.

Procedures

Preparation of tea and hops extracts

A specific mass of each tea or hops sample (see table in Appendix A for specifics) was dissolved separately in 100 mL of deionized (DI) water and boiled for 30 minutes. Samples were

then filtered into sterile 50 mL test tubes. Aliquots were taken from these test tubes, added to 1.5 mL microcentrifuge tubes, and centrifuged for 15 minutes at 10,000 rpm. Afterwards, the supernatant was removed and added to new 1.5 mL tubes. These tubes were frozen at -20°C.

ADH kinetics assay to determine rate of NADH production/consumption

Forward reaction kinetics

Yeast ADH favors the reduction of acetaldehyde to ethanol. This reaction consumes NADH and generates NAD+ (Figure 13). Therefore, an indirect way of measuring ADH activity is by detecting the amount of NADH consumed (and NAD+ produced), with greater amounts of NADH consumed correlating to greater ADH activity.

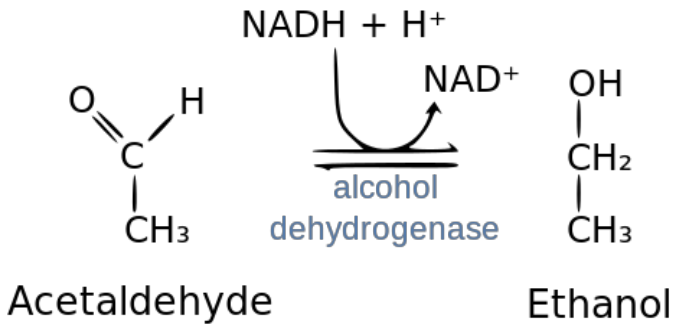

Figure 13: Yeast ADH converts acetaldehyde to ethanol to produce NAD+

Image obtained from: Biochemistry for Medics

Using a BioTek Instruments microplate-reader, transparent Corning 96-well plates, and Gen5 Version 1.11 (2005 BioTek Instruments) UV/Vis analysis software, ADH activity was determined based on the oxidation of NADH (absorbance at 340 nm) to NAD+ (no absorbance at 340 nm).

Sample preparation: In order to facilitate catechol-mediated modification of ADH, 15µL samples combining ADH and the catechol of interest were prepared and incubated. To prepare the ADH,

Dr. Landino treated it with a reducing agent to ensure that all cysteines were reduced. Excess reducing agent was removed by desalting on a gel filtration column. ADH concentration was determined by measuring its absorbance at 280 nm and consulting the Worthington Enzyme Manual to determine its E constant value at this wavelength, then using Beer's Law to calculate concentration. Our ADH was determined to be 2.36 mg/mL. This concentration was converted to molarity using the molecular weight of ADH, and this value was then used to calculate the volume of ADH required to produce a molarity of 10μM ADH in 15μL samples (2.16μL 2.36 mg/mL ADH). Because cysteines are the residues of interest, it is important to note the concentration of reactive cysteines in the sample. There are eight cysteines per ADH molecule (see Appendix C), thus a 10μM concentration of ADH results in a cysteine concentration of 80μM.

To create the samples, 2.16μL of ADH (2.36 mg/mL) was combined with 1.5μL of the catechol compound at varying concentrations. Catechol compounds used in this procedure include catechol, caffeic acid (CA), hydrocaffeic acid (HCA), and PP60. Concentrations tested include 1mM, 100μM, and 50μM compound in DI water. 1.5μL of mushroom tyrosinase was added to the sample to catalyze the transition of the catechol to ortho-quinone. The rest of the 15μL sample was 9.84μL of 0.1 M phosphate buffer pH 7.4 (PB).

Control 15μL samples included: ADH control consisting of just PB and 2.16μL ADH (to observe maximal ADH activity without modification) and tyrosinase control consisting of PB, 2.16μL ADH, and 1.5μL tyrosinase (to determine if tyrosinase itself has any effect on ADH activity). To observe the effects of catechol compounds on ADH activity independent of oxidation, samples without tyrosinase corresponding to each molecule type and concentration

were also prepared. All samples were incubated for 15 minutes to allow time for the catechol molecules to become oxidized and then modify ADH.

Plate preparation: After incubation, samples were diluted 1:30 (5µL sample + 145µL PB pH 7.4). Then, in a 96-well plate, the following was prepared:

	Column 1: Blank	**Column 2: Assay Control**	**Column 3: Sample 1**	**Column 4-N: Sample N**
Row A	200µL 20mM Tris buffer (pH 8.8)	190µL 20mM Tris buffer (pH 8.8) 10µL 10mM NAD+	165 µL 20mM Tris buffer (pH 8.8) 15µL 10mM acetaldehyde 10µL of 1:30 diluted sample 1 10µL 10mM NADH	165µL 20mM Tris buffer (pH 8.8) 15µL 10mM acetaldehyde 10µL of 1:30 diluted sample N 10µL 10mM NADH

The NADH was added at the end very quickly and carefully, as this is the component that initiates the reaction and is measured by the plate-reader to determine ADH activity. After the addition of NADH, individual wells were mixed with a 200 µL pipette and placed into the plate reader. For this procedure, the plate reader was kept at a temperature of 30°C. NADH absorbance was read every 30 seconds for 5 minutes at 340 nm. Using linear regression, the rates of NADH consumption in the antioxidant sample wells could be compared to that of the ADH control as an indirect measure of ADH activity.

Reverse reaction kinetics

The reduction of acetaldehyde to ethanol is a reversible reaction. Yeast ADH can also catalyze the oxidation of ethanol to acetaldehyde, and produce rather than consume NADH as a result (Figure 14). Thus, in this reaction, ADH activity is correlated to the amount of NADH produced.

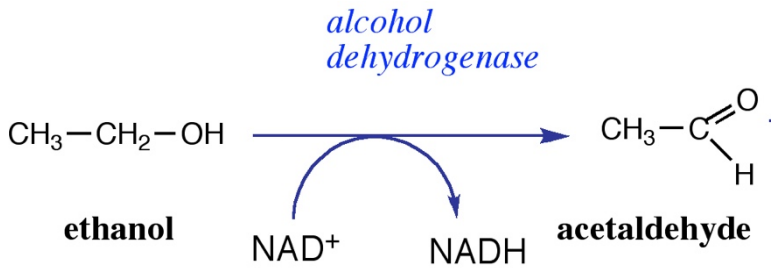

Figure 14: Yeast ADH converts ethanol to acetaldehyde to produce NADH

Image obtained from: Richard David Feinman

In this assay, ADH activity was determined based on the reduction of NAD+ (no absorbance at 340 nm) to NADH (absorbance at 340 nm), using the same equipment. Note differences in assay parameters from the forward reaction procedure.

Sample preparation: In order to facilitate catechol-mediated modification of ADH, 15µL samples combining ADH and the catechol of interest were prepared and incubated. 1.5 µL of ADH (2.43 mg/mL) was combined with 1.5µL of the antioxidant compound at varying concentrations. Catechol compounds used in this procedure include catechol, caffeic acid (CA), hydrocaffeic acid (HCA), and PP60. Concentrations tested include 1mM, 100µM, and 50µM compound in DI water. 2.0µL of a new sample of mushroom tyrosinase was added to the sample to oxidize catechol to ortho-quinone. The rest of the 15µL sample was 10µL of 10mM phosphate buffer pH 7.4 (PB).

Control 15µL samples included: ADH control consisting of just PB and 1.5µL ADH (to observe maximal ADH activity without modification) and tyrosinase control consisting of PB, 1.5µL ADH, and 2.0µL tyrosinase (to determine if tyrosinase itself has any effect on ADH activity). To observe the effects of catechol compounds on ADH activity independent of oxidation, samples without tyrosinase corresponding to each molecule type and concentration

were also prepared. All samples were incubated for 15 minutes to allow time for the antioxidant molecules to oxidize and modify ADH.

Plate preparation: After incubation, samples were diluted 1:50 (5µL sample + 245µL 10 mM PB pH 7.4). Then, in a 96-well plate, the following was prepared:

	Column 1: Blank	**Column 2: Assay Control**	**Column 3: Sample 1**	**Column 4-N: Sample N**
Row A	200µL 20mM Tris buffer (pH 8.8)	185µL 20mM Tris buffer (pH 8.8) 15µL 10mM NAD+	155 µL 20mM Tris buffer (pH 8.8) 15µL 1M EtOH 15µL of 1:50 diluted sample 1 10µL 10mM NAD+	155µL 20mM Tris buffer (pH 8.8) 15µL 1M EtOH 15µL of 1:30 diluted sample N 10µL 10mM NAD+

The NAD+ was added at the end very quickly and carefully, as this is the component that initiates the reaction and is read by the plate-reader to determine ADH activity. After the addition of NAD+, individual wells were mixed with a 200µL pipette and placed into the plate reader. For this procedure, the plate reader was maintained at 37°C. NADH absorbance was read every 30 seconds for 5 minutes at 340 nm. Using linear regression, the rates of NADH production in the antioxidant sample wells could be compared to that of the ADH control as an indirect measure of ADH activity.

Yeast sample preparation

Purpose: The ADH kinetics procedures measure the effects of catechol-based antioxidant compounds on isolated ADH activity *in vitro*. In order to measure the effects of these molecules on ADH in living yeast cells, yeast samples must be prepared and grown with the compounds. Instead of using NADH production or consumption as a basis to determine enzyme activity,

ethanol output of the yeast cells over time was measured and compared across samples grown with different compounds.

Sample preparation: To produce ethanol, yeast requires 'food' or glucose that will undergo glycolysis and produce pyruvate, which will then generate ethanol via anaerobic fermentation. The carbon source used in this procedure was dried malt extract (DME). A 10% solution of DME was created by mixing 2g DME power + 20mL DI water in a 125mL flask. In order to dissolve the powder and sterilize the solution, the flask was placed on a hot plate and the solution heated to boiling. To prevent moisture from evaporating from the flask and consequently increasing the concentration of DME past 10%, the flask was covered with aluminum foil and tightly sealed. The 10% DME mixture must be carefully watched as it is heated, and the heat must be turned down as soon as the solution starts to bubble (typically after about five minutes). This is to avoid any burning or evaporation of the solution.

In addition to a carbon source, yeast cells were mixed with catechol molecules so that the molecules may diffuse across cell membranes, theoretically modify ADH, and thus affect EtOH output as it is occurring. Each compound was prepared at 2mg/mL, and the solution was then vortexed until all the powder dissolved. It is important to note that caffeic acid (CA) is not soluble in room temperature water, and therefore the compound must be heated to dissolve. All compound solutions were heated to sterilize. 2mg/mL compounds give a molarity of about 1.85M in the final yeast sample for both CA and HCA. The molarity cannot be determined for PP60 because it is composed of many different molecules with varying molecular weights.

Once the DME and catechol compounds were prepped, 2mL yeast samples were prepared in sterile test tubes. To make this sample, the following was added to the test tube (in order): 1.5mL 10% DME, 333µL 2 mg/mL compound, 167µL yeast (either SafAle-05 or BS 565). The

DME was added using a sterile plastic pipette, while the yeast must be pipetted using sterile autoclave tips to minimize the risk of contamination. Before being added to the sample, yeast cells were resuspended with the vortex, then pipetted up and down four times to ensure even distribution. Three separate samples were prepared for each compound of interest to serve as different trials. For example, if a given experiment were to test the effects of CA and hydrocaffeic acid (HCA) on yeast ADH activity, three 2mL samples would be made with CA and three with HCA. In each experiment, control samples were made by adding 333µL DI water to provide a standard for EtOH output without the interference of catechol molecules on ADH activity (Figure 15). The final concentration of catechol molecule in the samples was about 1.85mM for both CA and HCA. After preparation, samples were stored in the dark (i.e. in a cabinet) and the tubes were not shaken to provide anaerobic conditions.

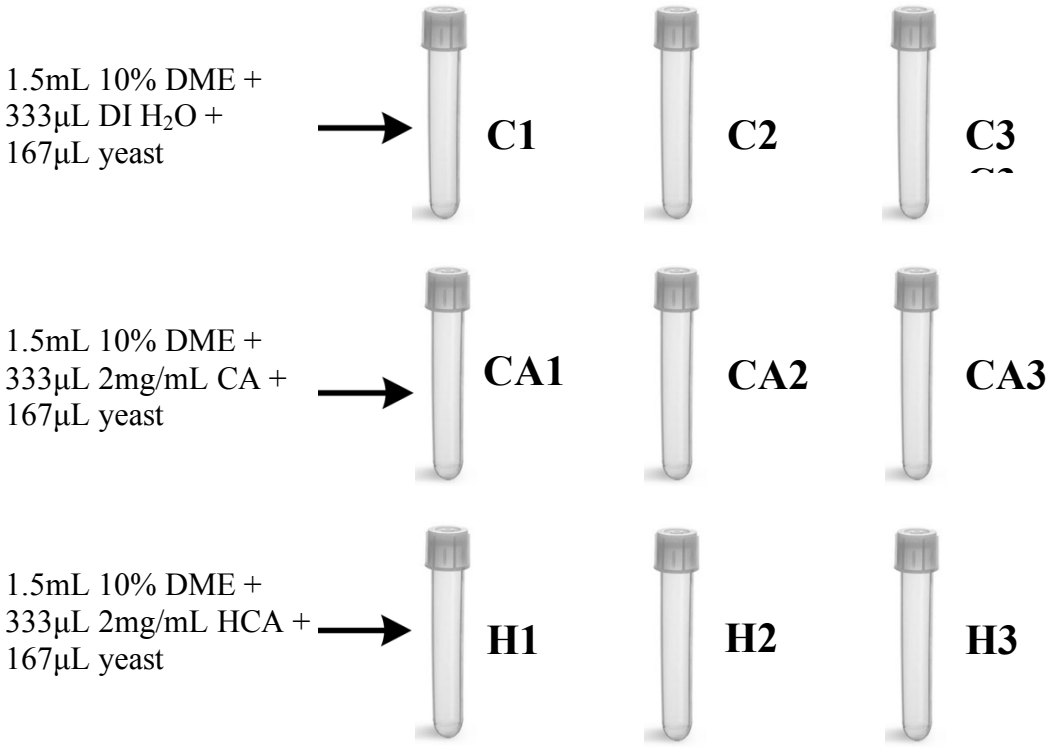

Figure 15: An example of yeast sample set-up, with each compound represented by 3 separate samples.

Sample extraction: To ultimately measure EtOH output of the yeast cells over time, extracts were removed from each sample at even time intervals stipulated by the specific experiment. For preliminary experiments, the specified time interval was 24 hours for the four days following sample preparation. Later on, extracts were removed every 12 hours for the two days following sample preparation (with the time of sample creation being t = 0 hours). Extracts consisted of 100μL aliquots taken from the supernatant, avoiding the inclusion of yeast cells as best as possible. These aliquots were transferred to 650μL microcentrifuge tubes, each labeled with the compound/sample number and day or hour of extraction. It is important to note that samples from the same compound were not combined. That is, for every time interval, the same number of microcentrifuge tubes were used as sterile test tubes containing the original samples. Extracts were stored in the freezer to ensure that any yeast cells that remained in the aliquot were unable to continue to produce ethanol.

MTT/PMS kinetics assay to determine [EtOH] in yeast supernatant

Purpose: In the ADH kinetics assay, the rate of the ADH reaction is assessed by measuring NADH consumption or production during the reaction based on its absorbance at 340 nm. To measure ADH activity in living yeast cells, however, NADH absorbance cannot be used as the measurement parameter because it must be observed in real-time as the reaction is occurring. Therefore, ethanol output in terms of final ethanol (EtOH) concentration was used to determine ADH activity at the time the reaction occurred, with higher [EtOH] corresponding to greater ADH activity. The unknown concentration of ethanol was determined in this procedure using the reduction properties of NADH and the absorbance of MTT.

Background: ADH catalyzes the reversible reaction of ethanol to acetaldehyde, and in doing so reduces NAD+ to NADH. EtOH and NAD+ react in a 1:1 ratio, yielding a concentration of

NADH equal to that of the EtOH reacted. Thus, one way to determine the amount of EtOH in yeast supernatant is to add ADH and NAD+ and observe the formation of NADH to completion.

However, ADH favors the reverse reaction (acetaldehyde to EtOH), therefore the formation of NADH fails to go to completion on its own, and some of the EtOH remains unreacted. As such, simply reading NADH absorbance at 340 nm is insufficient to determine total [EtOH]. To drive the ethanol to acetaldehyde reaction to completion, this procedure takes advantage of LeChatelier's principle and couples the reaction with MTT/PMS.

The two electrons in NADH are passed from PMS to MTT, ultimately reducing MTT to a blue-colored molecule called formazan, the absorbance of which can be read at 630nm. This drives the ethanol to acetaldehyde reaction to completion in accordance with LeChatelier's principle (Figure 16).

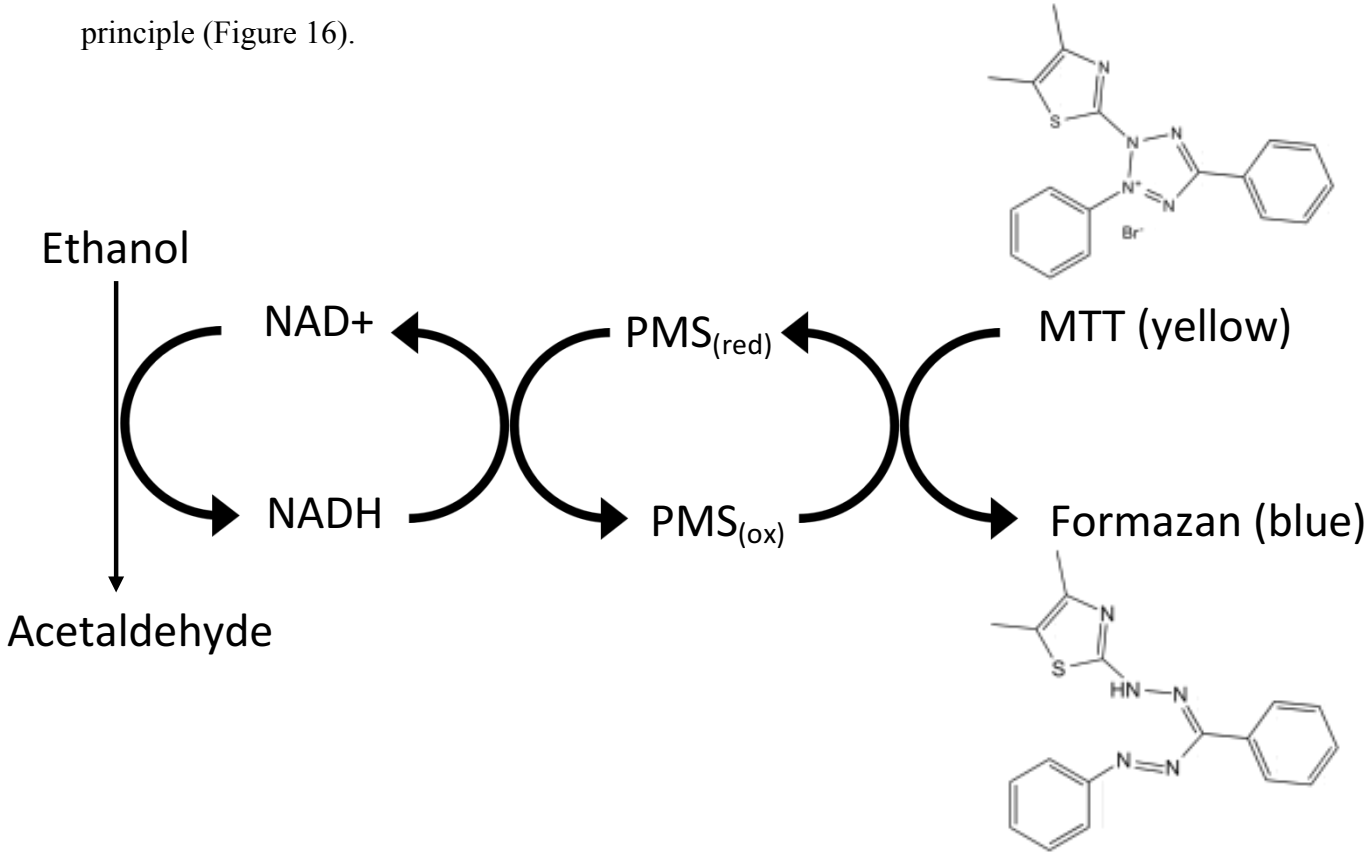

Figure 16: The ADH-catalyzed reaction of ethanol to acetaldehyde produces NADH in a 1:1 correspondence with the original amount of EtOH. The electron in reduced NADH can be shuttled through PMS and ultimately to MTT (also in a 1:1 ratio). MTT is reduced to formazan, a blue molecule whose absorbance can be read at 630 nm. This drives EtOH oxidation to completion.

Molecule images obtained from: Dojindo

Because MTT reduction occurs at a 1:1 ratio with NADH consumption, the concentration of formazan formed and ethanol consumed at completion are equivalent. Using Beer's Law (see below), the absorbance of MTT at 630 nm can be used to determine its concentration, which ultimately determines the unknown [EtOH] in solution.

A standard EtOH solution with a known concentration of 150µM EtOH was used to confirm the viability of the procedure. The standard also serves as a reference for comparison with the unknown samples. The absorbance at 630 nm for 150uM MTT (and thus, EtOH) should be approximately 0.48. See the following use of Beer's law for explanation:

A=(ε*b*c) where ε is the extinction coefficient for NADH (6220 M-1 cm-1), b is the pathlength (previously determined by Lydia Boike to be 0.51 cm), and c is the concentration of EtOH

So, in the case of the standard 150uM EtOH solution:

A=(6220*0.51*150e^(-6))

A = 0.476

Thus, absorbance in the case of the standard EtOH solution, should be approximately at 0.48 when reaction is at completion.

Plate preparation: In this procedure, samples were mixed directly in the 96-well plate, incubated to allow for the reaction to occur, then a MTT/PMS solution was added to each well directly prior to insertion in the plate reader. Before plating, supernatant extracts taken over the course of

several days were thawed and diluted 1:100 in DI water. These diluted extracts served as the "samples" in this experiment.

The first row in any given experiment provided a "baseline" absorbance for the reactions prior to the addition of MTT/PMS. This accounts for any absorbance that constituents of the reaction themselves contribute to the absorbance at 630nm. Because absolute final absorbance value is needed to determine [EtOH] (unlike ADH kinetics, which assessed relative rates of reaction), the baseline reaction absorbance is subtracted from the final absorbance values of the other reactions stained with MTT/PMS. With this in mind, plate set-up was as follows:

	Column 1: Blank	**Column 2: EtOH standard**	**Column 3: Sample 1**	**Column 4-N: Sample N**
Row A ("baseline")	200µL 20mM Tris buffer (pH 8.8)	149.48µL 20mM Tris buffer (pH 8.8) 15µL ADH (0.324mg/mL) 5.52µL 5% std 30µL 10mM NAD+	149.48µL 20mM Tris buffer (pH 8.8) 15µL ADH (0.324mg/mL) 5.52µL sample 1 30µL 10mM NAD+	149.48µL 20mM Tris buffer (pH 8.8) 15µL ADH (0.324mg/mL) 5.52µL sample N 30µL 10mM NAD+
Row B: Time interval 1 (i.e. Day 1)	200µL 20mM Tris buffer (pH 8.8)	89.48µL 20mM Tris buffer (pH 8.8) 15µL ADH (0.324mg/mL) 5.52µL 5% std 30µL 10mM NAD+	89.48µL 20mM Tris buffer (pH 8.8) 15µL ADH (0.324mg/mL) 5.52µL sample 1 30µL 10mM NAD+	89.48µL 20mM Tris buffer (pH 8.8) 15µL ADH (0.324mg/mL) 5.52µL sample N 30µL 10mM NAD+

Note that each row contains the extracts taken at a specific time interval. That is, row B represents time interval 1 (i.e. Day 1), row C represents time interval 2 (i.e. Day 2), etc.

Once the reactions were prepared in the plate, the entire plate was incubated at 37 °C for 15 minutes. During this incubation time, the MTT/PMS redox dye mixture was prepared. In this procedure, the MTT/PMS solution was made in a 1:1 ratio. That is, 500µL of 1mM MTT was combined with 500µL of 1 mM PMS for a final concentration of 500µM for each compound. Other experimenters that have used this procedure for similar purposes have used PMS at a much lower concentration than MTT, typically in a ratio of 1:10. However, for this particular instance, repeated trials at varying concentrations of each compound demonstrated that equal concentrations of MTT and PMS is optimal for driving the ethanol to acetaldehyde reaction to completion.

Kinetics assay: The same BioTek plate reader and Gen5 analysis software used in the ADH kinetics assay procedures was used in this experiment. Upon removal from the incubator, 60µL of the 1:1 MTT/PMS mixture was quickly added to each sample well (not including the 'baseline' samples from Row A). After the redox dye was added, each sample well was mixed using a 200µL pipette and the plate was inserted into the plate reader. The reader was set to 37°C for this experiment, and collected data every 5 minutes for 3 hours, or until the absorbance plateaued. The final absorbance value at 630 nm was used to calculate the original concentration of ethanol from the yeast supernatant sample, assuming the 1:1 ratio of electron transfer. All calculations were made using Beer's Law, as described above.

MTT/PMS assay to compare rate of oxidation

The MTT/PMS assay determines [EtOH] by reacting the reduced NADH that is formed in the ADH-catalyzed reaction of ethanol to acetaldehyde with oxidized PMS to form reduced

PMS. Reduced PMS then passes the electrons on to oxidized MTT and reduces it to purple formazan.

$$NADH_{red} + PMS_{ox} \rightarrow NAD+_{ox} + PMS_{red}$$

$$PMS_{red} + MTT_{ox} \rightarrow PMS_{ox} + MTT_{red} \text{ (purple)}$$

In this reaction series, NADH serves as a reduced reagent that transfers its electrons on to PMS and ultimately to MTT. As such, it can be replaced by other reduced compounds (such as catechol-based molecules) that will then undergo the same reaction sequence. In this case, the rate of formazan formation corresponds to the rate of oxidation of the compound. This is a useful procedure in comparing relative rates of oxidation among the catechol compounds studied with ADH.

In the ethanol detection assay, EtOH, ADH, and NAD+ were needed to form the reduced NADH in the samples. However, when detecting oxidation rates of catechol compounds, just the compound is added as it already exists in its reduced form. Thus, plate set-up is as follows:

	Column 1: Blank	**Column 2: compound 1**	**Column 3: compound N**
Row A	200µL 20mM Tris buffer (pH 8.8)	110µL 20mM Tris buffer (pH 8.8) 30µL 10µM compound (or 2mg/mL in the case of PP60)	110µL 20mM Tris buffer (pH 8.8) 30µL 10µM compound (or 2mg/mL in the case of PP60)

The BioTek plate reader was run at 37°C for approximately 80 minutes, or until the curves leveled off. The oxidation rate of each molecule was then plotted versus absorbance at 630 nm over time.

Native gel procedure to determine structural and functional protein modifications

Purpose: The ADH kinetics and MTT/PMS assays examined purified and living cell ADH activity respectively. It is of use to explore *how* the catechol compounds are affecting ADH activity; that is, what structural modifications are the molecules making to the protein itself? This gel electrophoresis technique was used to investigate conformational (and activity) changes in ADH.

Background: Gel electrophoresis is a technique used to separate proteins based on charge and size, with larger, heavier proteins travelling slowly through the gel and smaller proteins running quickly to the end. Denaturing gel electrophoresis techniques use the detergent sodium dodecyl sulfate (SDS) and a reducing agent in the sample loading buffer to render the charge of the proteins negligible and separate them based solely on molecular weight or size. To avoid denaturing the protein while still detecting structural differences, native gel electrophoresis is used. This procedure does not involve SDS, a reducing agent, or heat, and is useful in isolation of enzymes and studying protein complexes (Braz & Howard, 2009). Thus, native gel electrophoresis is of greater use in this experiment to determine if the enzyme ADH was modified, while still preserving its potential for activity.

Sample preparation: The samples to be run in the gel included ADH control and ADH combined with the catechol molecule of interest. This allowed for observations in 'band' and thus structural differences between control versus modified ADH. Samples were prepared as follows:

Sample	**ADH**	**Buffer**	**Compound**	**6xSB: Sample buffer (glycerol + bromophenol blue) – added after incubation**
1	2.16µL	12.84µL 10mM PB(pH 7.4)		3µL

2 - N	2.16µL	10.84µL 10mM PB(pH 7.4)	2.00µL 10mM catechol compound	3µL

After preparation, samples were incubated for 15 minutes to allow time for the catechol molecules to modify ADH. Before loading into the gel, 3µL of 6xSB was added to each sample.

Gel preparation: The gel itself was made from 0.8% agarose. 0.32g of agarose were weighed and added to 40mL of 20mM Tris (pH 8.6) 2 mM EDTA 20 mM glycine (prepared by Dr. Lisa Landino) in a 125mL flask. The mixture was then microwaved in 5-10 second intervals until the agarose dissolved in solution, with extra care taken to avoid allowing the solution to boil over.

While allowing the agarose solution to cool, the plastic gel frame was assembled by attaching rubber stoppers to either end of the frame and placing the comb centered on one end, with the 8-tooth side facing down. At this point, the gel was poured into the frame and left for 20 minutes to solidify. Once solid, the comb was removed by carefully pulling straight up and the rubber stoppers removed cautiously to avoid making any tears in the gel. The frame was then placed into the electrophoresis system, and the apparatus filled with 260mL of 20mM Tris (pH 8.6) 2 mM EDTA 20mM glycine. Note: for ADH at this pH, the protein will run toward the cathode, so it is important to arrange the gel so that the wells are on the anode (left) side of the apparatus.

Running the gel: After sample solutions were mixed and the gel was placed in the electrophoresis system, samples were pipetted into their respective wells. To ensure that all of the sample was pipetted, the pipette was set to 1µL more than the sample volume (that is, the 18µL samples were pipetted using 19µL pipette). The cover was then placed on the electrophoresis apparatus, and turned on. ADH was run at 90 volts for 90 minutes, or until the bromophenol blue reached the end of the gel.

Gel development: While the gel was running, a development solution was made to ultimately be used to stain the gel bands for easier visualization. To make the solution, the following was combined in a 125mL flask: 10mL 0.2M Tris (pH 8.6), 10mL DI water, 8-10mg NAD+ (~0.75mM), 28µL EtOH (~25mM), 3-5mg NBT, and 1mg PMS.

Once the gel was done running, it was carefully removed from the apparatus, placed into a plastic container, and covered with the development solution. The container was then placed on the multi-purpose rotator for approximately 10 minutes. Because the development solution is light-sensitive, a Styrofoam cover was positioned over the gel container to keep it dark. Once the gel had developed, the solution was poured out of the container and the gel rinsed with water. The colorimetric protocol of the Bio-rad Gel imager was used to photograph the gel. Darker bands indicate higher levels of ADH activity, and bands in different lateral positions on the gel suggest differing protein structures or conformational changes.

RESULTS AND DISCUSSION

Relative oxidation rates of ortho-quinone molecules

Catechol molecules are able to undergo a Michael addition when they are oxidized to ortho-quinones. Thus, molecules that oxidize at a quicker rate are also expected to react with the nucleophile at a quicker rate. In this biological context, where the nucleophile is a cysteine residue in ADH, this suggests that catechol molecules that oxidize more quickly are more likely to modify (and theoretically inhibit) ADH.

Relative oxidation rates of different catechol compounds were assessed using the MTT/PMS assay. The rate of formazan formation (absorbance at 630 nm) directly corresponds to the rate of catechol oxidation. The experiment was repeated three times for each molecule.

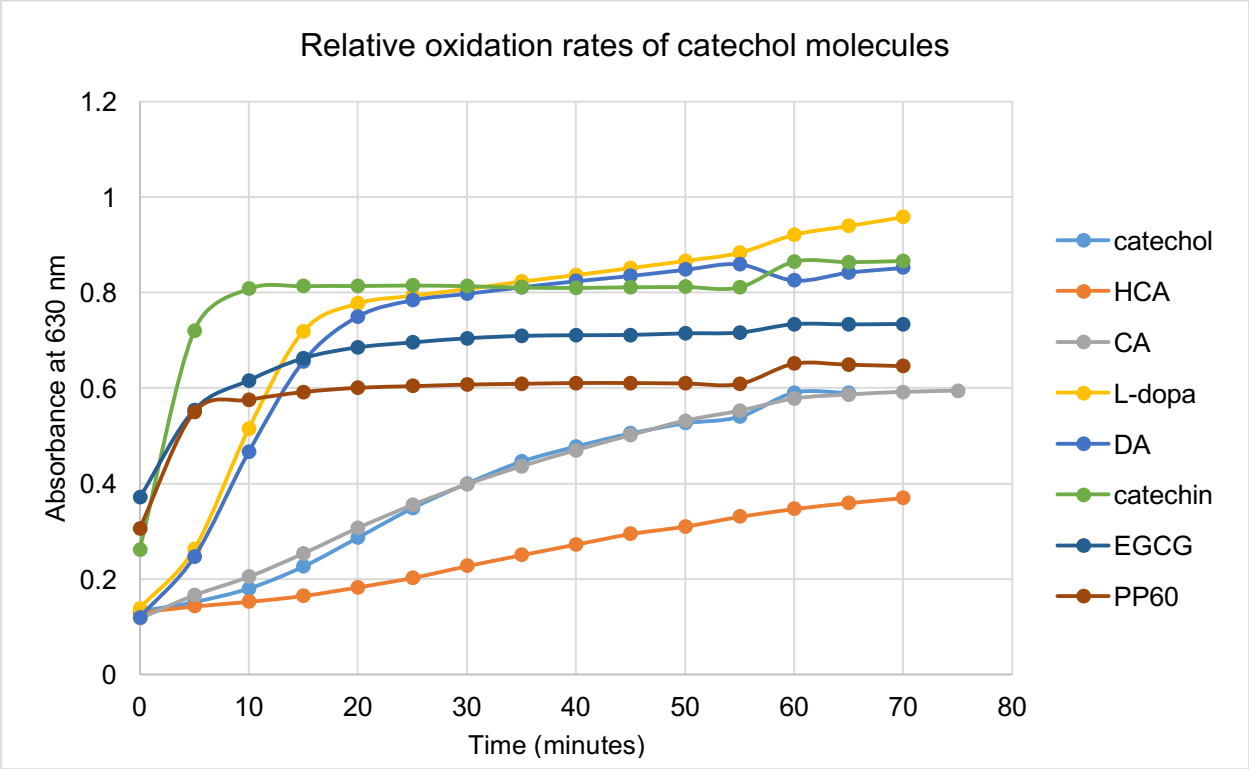

Figure 17: The oxidation rates of the above molecules were determined using the MTT/PMS assay outlined in the methods sections. Oxidation rate can serve as an indicator of how readily the molecule reacts with and modifies ADH. All samples were made at 10mM, with the exception of PP60 at 2mg/mL.

It is of interest to note the shapes of the curve of each molecule in relation to its chemical structure. For instance, catechol, HCA, and CA all share very similar chemical structures, and their oxidation rates follow similar patterns. Epigallocatechin gallate (EGCG) is the primary constituent of the mixture PP60, and these molecules also follow similar paths. Similarly, L-dopa and dopamine (DA) have almost identical structures, and oxidize in almost identical fashions. The only molecule tested that is structurally unique was catechin, and it has its own unique oxidation curve. The chart can thus be interpreted based on these groupings, with molecules of similar chemical structures following similar oxidation paths.

The oxidation rate of the catechol molecules is relevant in that it putatively affects the extent to which the molecule affects ADH activity. The proposed mechanism for catechol modification of ADH involves oxidation of the catechol to a quinone, which then undergoes a

Michael addition with vulnerable cysteines serving as nucleophiles. Thus, it logically follows that, with other structural specificities conserved (i.e. in the case of CA and HCA), molecules that oxidize more quickly are likely to inhibit ADH to a greater extent. Unlike the enzyme kinetic assays, this assay did not use tyrosinase to oxidize the catechols, but rather relied on air oxidation over time. This is relevant in a mammalian system, where air is much more likely to be present and able to oxidize molecules than a mushroom enzyme.

Detecting the inhibition of isolated ADH using enzyme kinetic assay

Reverse reaction kinetics

Initial experiments testing the effects of o-quinones on ADH activity were done using isolated ADH to facilitate the reverse reaction of ethanol into acetaldehyde, thus producing NADH. Oxidation of the catechols was catalyzed using mushroom tyrosinase enzyme, indicated by "E" in the results charts. The activity level of each sample is represented as a bar standardized to the activity of the ADH control sample. That is, 100% indicates full ADH activity, and bars approaching 0% (lower bars) indicate less ADH activity, or greater inhibition. The following is a comprehensive report of the catechol molecules tested and their effects on ADH activity. Molecular structures of the catechols tested are included, and a complete chart including their structures and additional information can be found in Appendix A.

Catechol

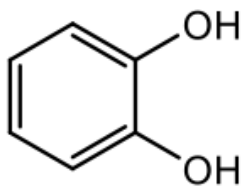

Catechol, the base molecule for all other derivatives tested, consists only of a benzene ring with two adjacent hydroxyl groups attached. Catechol is present in a wide variety of plants, namely onions, apples, crude beet sugar coal, oak, and willow trees.

As a general note, ADH is present at 10µM concentration in the samples, therefore the cysteines have a concentration of 80µM. The concentrations of the catechol molecule in these experiments were chosen because they are close to the enzyme concentration. We are interested in the ratio of the damaging reagent (i.e. catechol or a catechol derivative) to the reactive group (in this case, cysteines). A smaller ratio suggests that the damaging reagent is having a real, plausible effect on the system. For example, if there is 1000 times more catechol than ADH in a sample, it would not be surprising if ADH activity was drastically impacted, but this would also not tell us much, practically speaking.

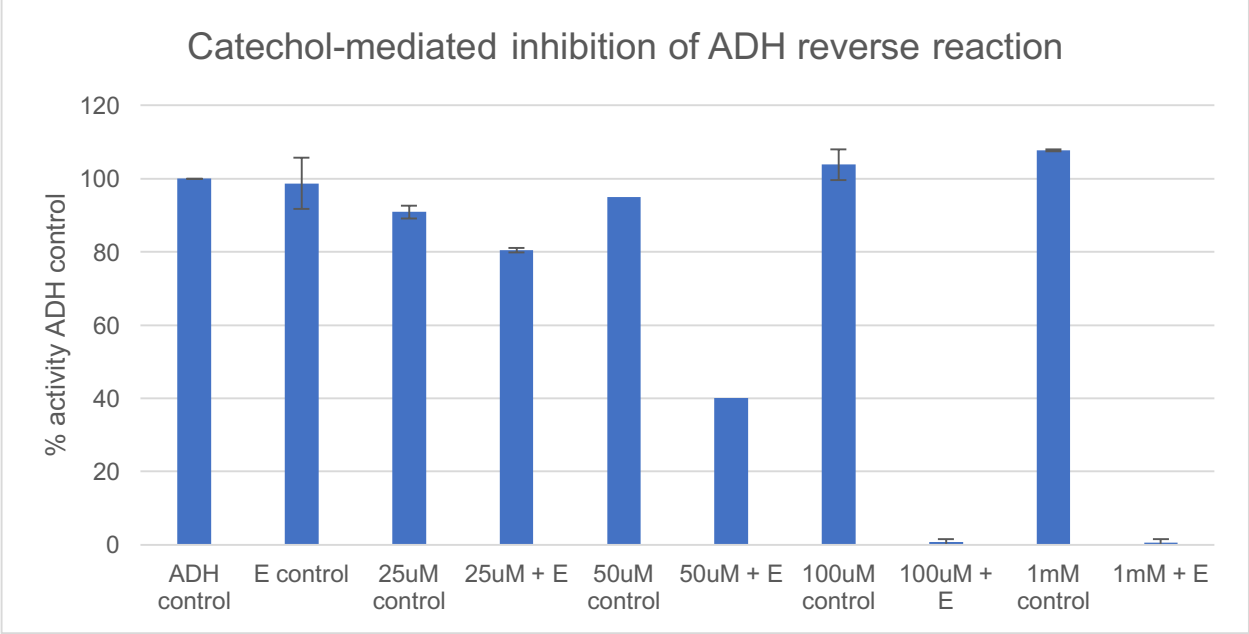

Figure 18: Samples above combined ADH and catechol at concentrations 25µM, 50µM, 100µM, and 1 mM. E indicates the sample also included tyrosinase. Shown above are the averages across three trials.

The above results demonstrate the concentration-dependent inhibition of ADH by catechol. Complete inhibition of ADH is only seen at 100µM and 1mM concentrations, thus indicating that ADH is less sensitive to catechol at very low concentrations. At every

concentration of catechol, the addition of tyrosinase was required to see inhibition (though this effect is seen much more dramatically at the higher concentrations). This matches the expectation, as tyrosinase expedites the rate of oxidation, thus there are more oxidized molecules available to react with the nucleophilic cysteines of ADH.

Hydrocaffeic acid and caffeic acid

Hydrocaffeic acid (HCA) is found in many different plants, including coffee and artichoke leaves.

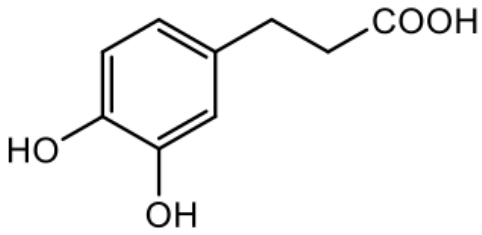

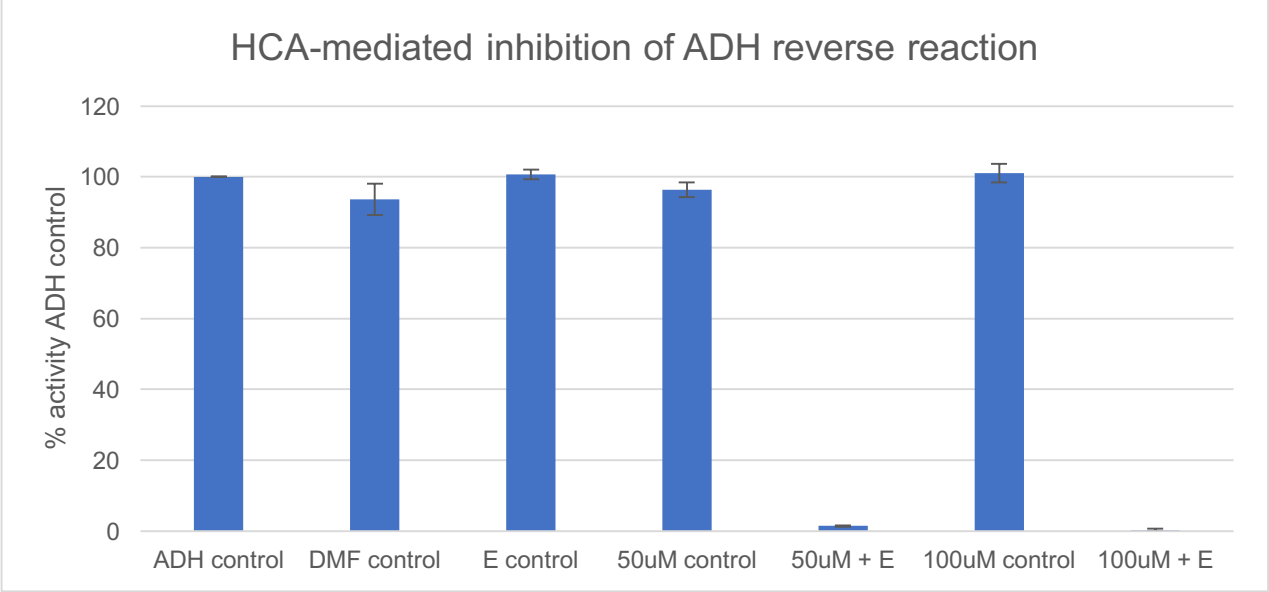

Figure 19: Samples above combined ADH and HCA at concentrations 50µM and 100µM. A DMF control is also included as HCA was being dissolved in DMF at this stage in the research. Shown above are the averages across five trials.

Similar to catechol, these results demonstrate the need to oxidize the molecule in order to observe the inhibitory effects, thus strengthening the Michael addition hypothesis. Unlike catechol, HCA is able to inhibit ADH at lower concentrations (i.e. 50µM). Thus, it was not necessary to test the higher concentration of 1mM HCA.

Caffeic acid (CA), a molecule present in all plants, is almost identical in structure to HCA, with the exception of a double bond between carbons two and three of the carbon chain substituent. Thus, it can be reasonably expected that the effects of CA on ADH activity closely resemble those of HCA.

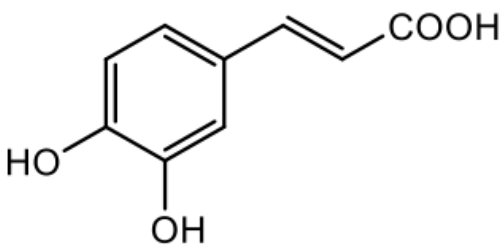

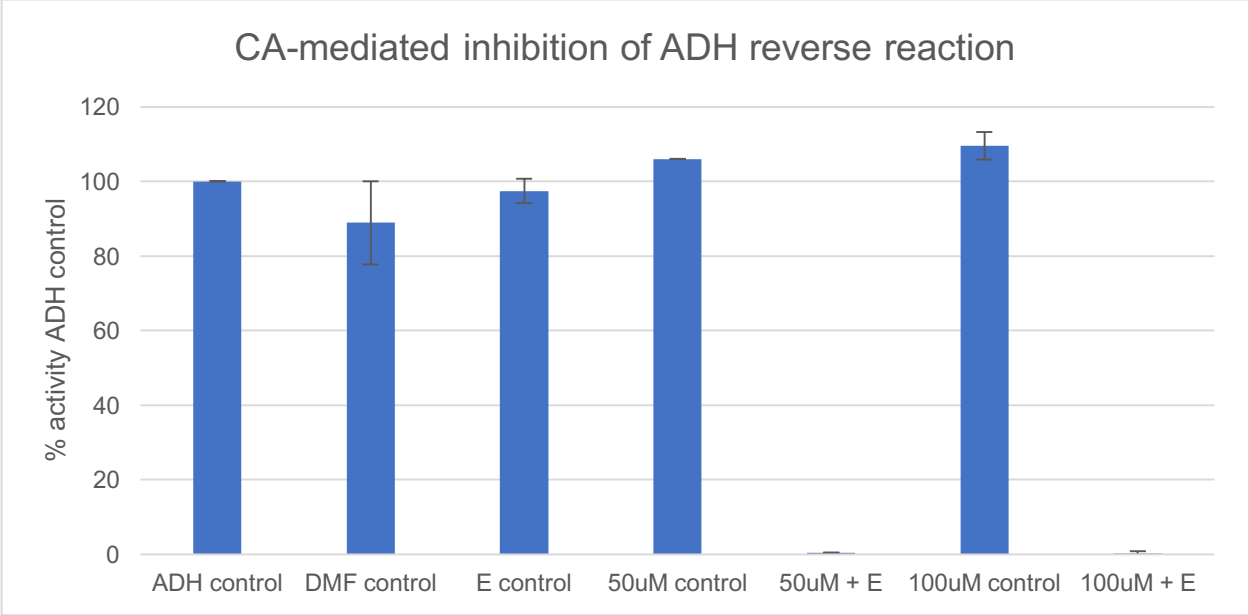

Figure 20: Samples above combined ADH and CA at concentrations 50µM and 100µM. A DMF control is also included as CA was being dissolved in DMF at this stage in the research. Shown above are the averages across five trials.

As pictured in the chart above, the results match expectation. Like HCA, oxidized CA in its quinone form completely inhibits ADH activity, even at lower concentrations.

L-tyrosine and L-dopa

Continuing the trend in increasing complexity of molecular structure, L-tyrosine and L-dopa were studied. It is important to note that L-tyrosine is not a catechol derivative, as it consists of only one hydroxyl group directly attached to the benzene ring. L-tyrosine is of interest to study because it is a precursor to L-dopa, which in turn is a precursor to dopamine, a

ubiquitous neurotransmitter. Furthermore, L-tyrosine is present in plants including seaweed, pumpkin leaves, spinach, and beans, as well as in animal-based products. In fact, the name of the enzyme "tyrosinase" is derived from its ability to oxidize tyrosine, the process responsible for the blackening of a skinned or peeled potato.

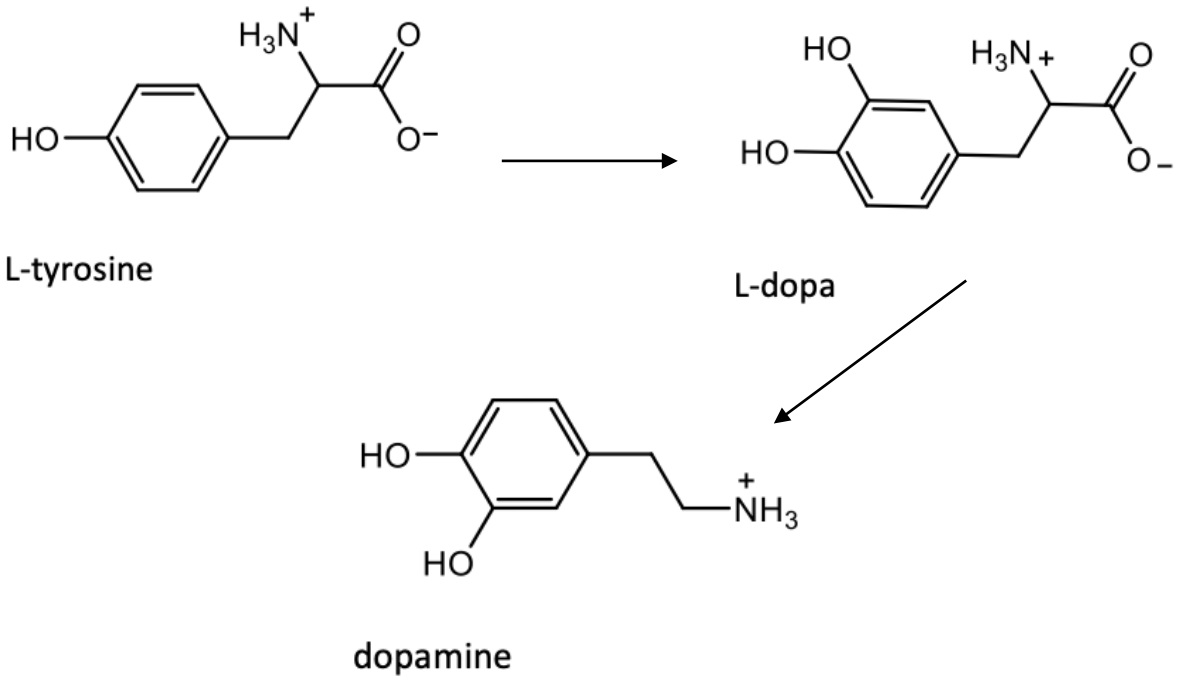

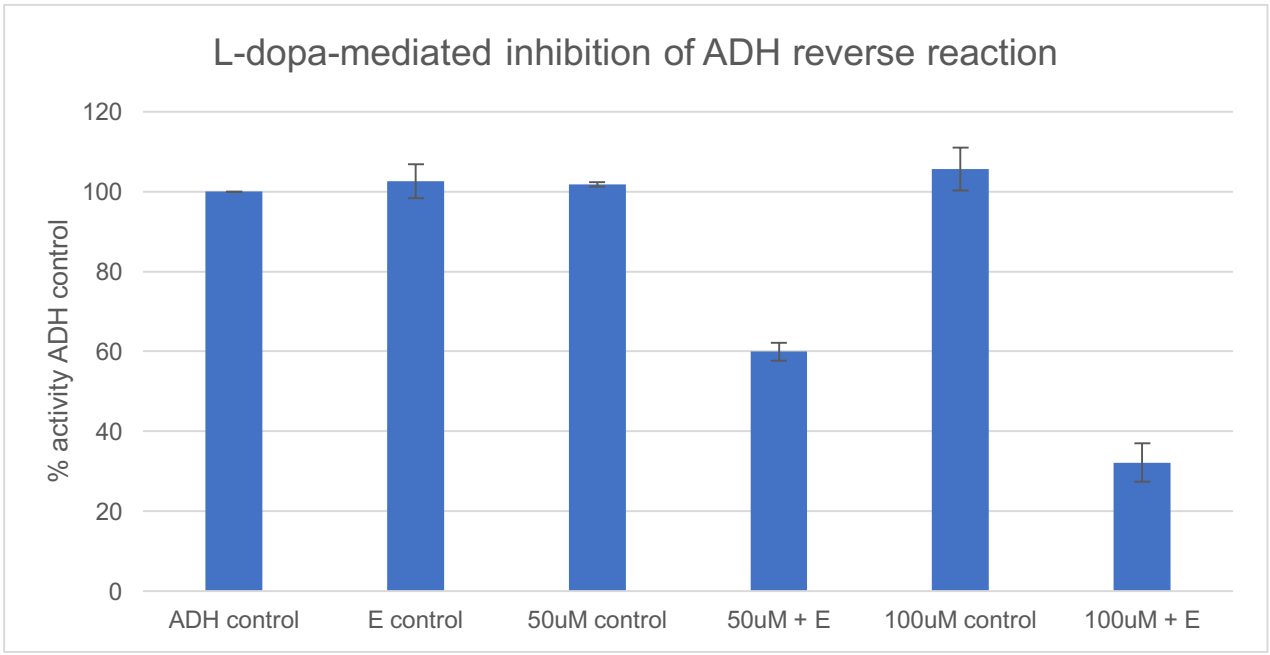

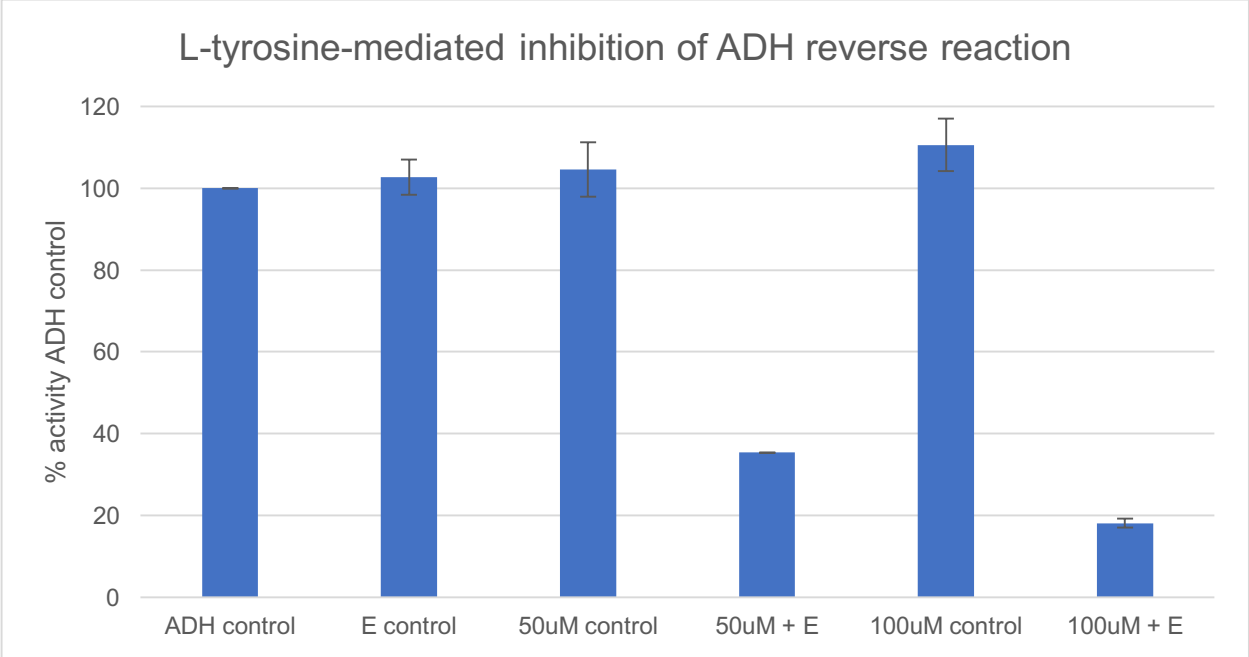

Figure 21: Top: Molecular structures of L-tyrosine, L-dopa, and dopamine. Arrows indicate the order of conversion of L-tyrosine to dopamine. Bottom: Samples above combined ADH and L-tyrosine/L-dopa at concentrations 50μM and 100μM. Shown above are the averages across three trials.

Oxidized L-tyrosine and L-dopa also demonstrate the ability to inhibit ADH activity; however, not to the same extent as HCA and CA. All samples still maintain some level of ADH activity, in contrast with the complete inhibition seen in the tyrosinase-catalyzed HCA and CA samples. We speculate that this may be due to the increased structural complexity of the molecule and thus lesser accessibility to electrophilic carbons for the Michael addition. In particular, oxidized dopamine is able to react with itself and form a cyclic compound, with the nitrogen of the amine group serving as the nucleophile. By definition, intramolecular reactions are always faster than intermolecular reactions, and furthermore, ADH is a much bigger molecule than dopamine, rendering the cysteines more difficult to access. Thus, the reactive cysteines of ADH are likely to be outcompeted by dopamine itself, and the integrity of the enzyme is maintained.

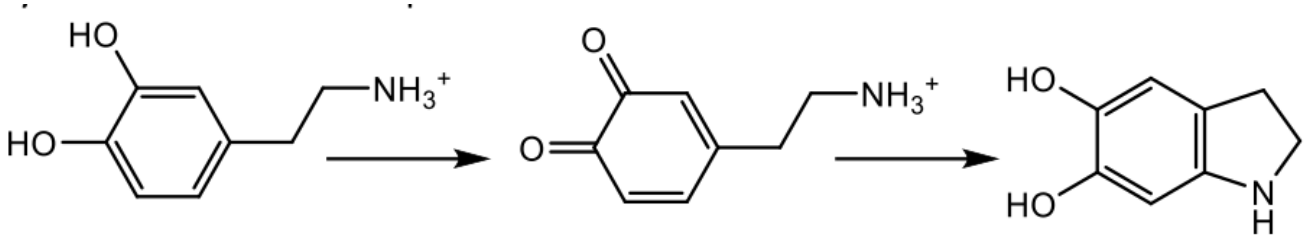

Figure 22: Tyrosinase oxidation of dopamine and intramolecular Michael addition

Other compounds that were tested with ADH include gallic acid, alizarin, quercetin, and morin. All of these molecules are more complex in structure than those previously listed (refer to Appendix A), and do not demonstrate the ability to inhibit ADH at lower concentrations.

Polyphenon 60

Polyphenon 60 (PP60) is an extract which contains a mixture of polyphenolic compounds found in green tea known to have antioxidative properties. The specific contents of the extract include 60% catechin derivatives, comprised of: 34% (-)-epigallocatechin-3-gallate (EGCG), 16.7% (-)-epigallocatechin, 8.7% (-)-epicatechin-3-gallate, 7.3% (-)-epicatechin, 2.8% (-)-gallocatechin gallate, and 0.5% (-)-catechin gallate, tannic acid, or (-)-epigallocatechin-3-gallate.

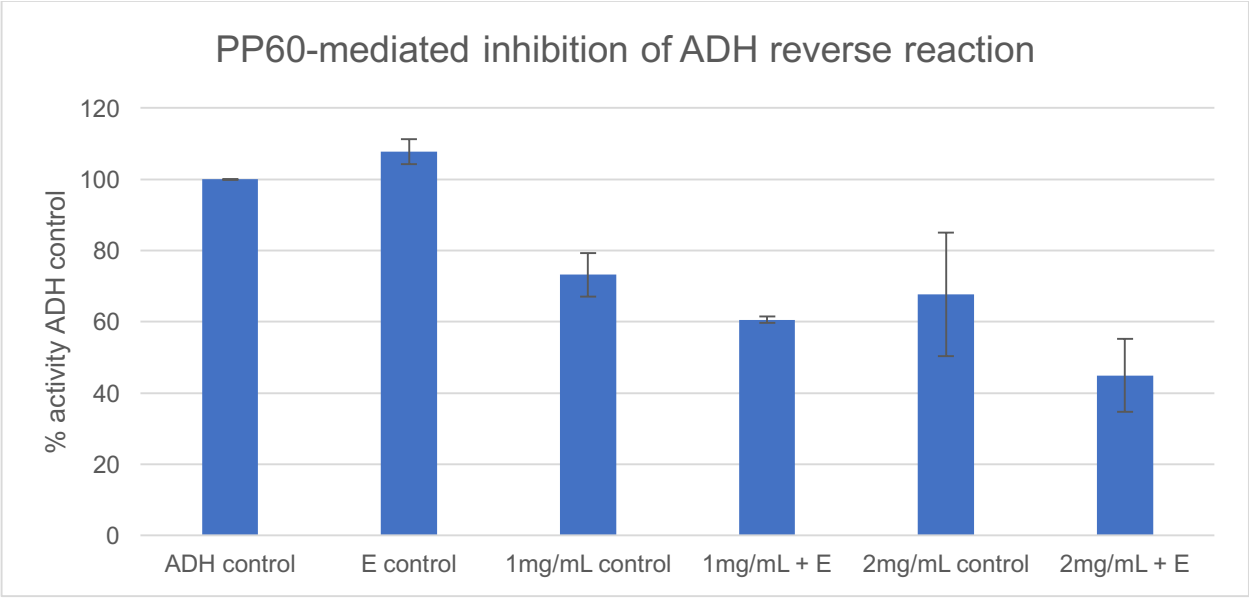

Figure 23: Samples above combined ADH and PP60 dissolved at 1 mg/mL and 2 mg/mL. Specific molarity for PP60 cannot be determined as it consists of many different molecules with different molecular weights. Shown above are the averages across three trials.

Like L-tyrosinase and L-dopa, PP60 did not completely inhibit ADH activity, even with oxidation catalyzed by tyrosinase. It is of interest to note, however, that the addition of tyrosinase did not dramatically increase the effect of PP60 on ADH as it did on the individual compounds. It is possible that because of the increased number of compounds present in solution, there is likely to be an increased number of oxidized molecules. Perhaps these molecules react with each other rather than ADH, thus reducing the impact they have on its activity.

Tea extracts and hops extracts

The compounds and extracts tested above are of interest to the scientist that is able to purchase the powders from chemical companies online; however, they are of less interest to the consumer that does not ingest pure caffeic acid but rather seeks to understand how these molecules become physiologically relevant in the food and drink he or she consumes. Thus, we created extracts of various types of teas and hops compounds (found in beer) that one may purchase at a grocery store and tested the effects of these extracts on ADH activity.

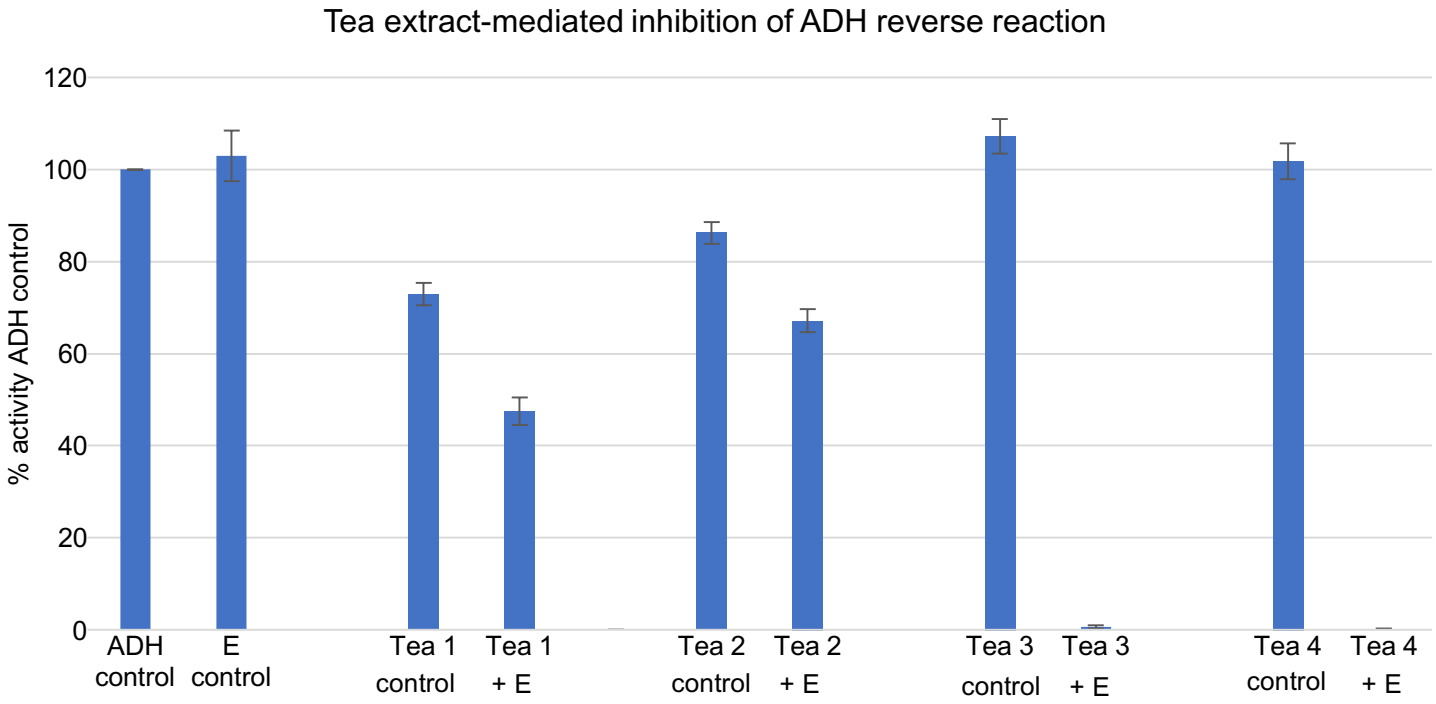

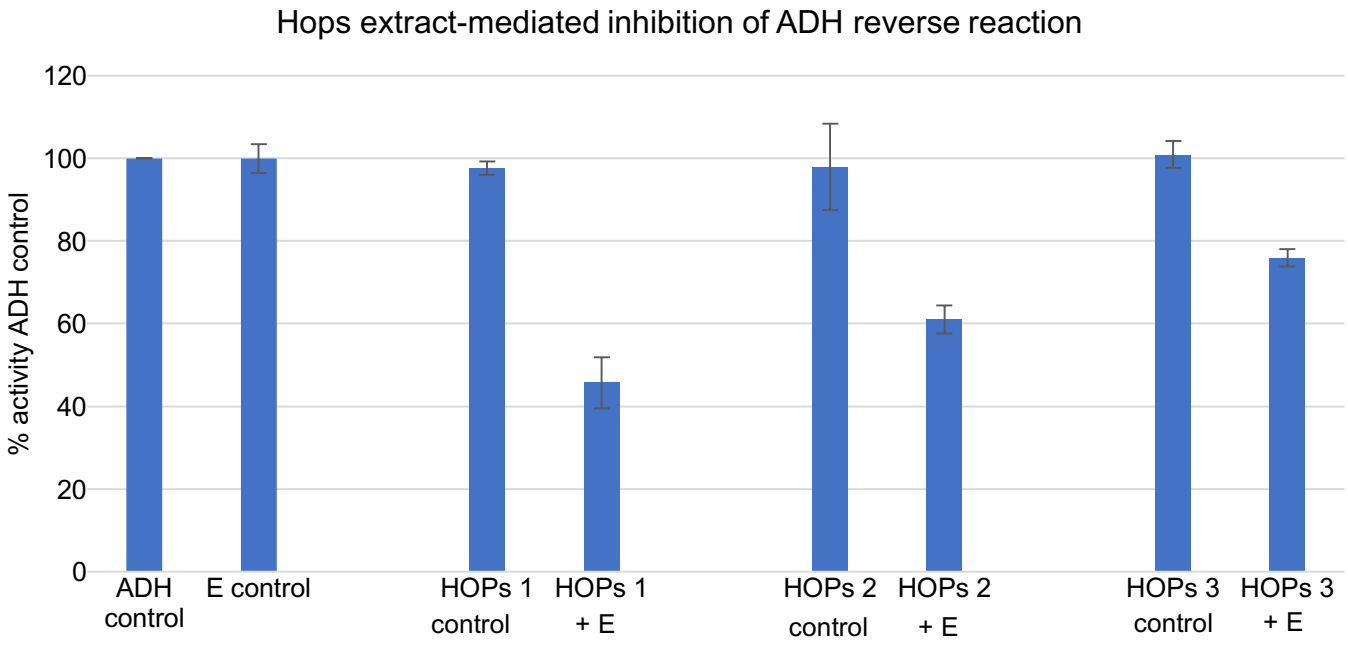

Figure 24: Samples above combined ADH and tea/hops extracts. The extract was not diluted before being mixed into the sample. Though labeled as Teas 1-4 and Hops 1-3 in these graphs, the specific tea and hops brands can be found in Appendix A. Shown above are the averages across three trials.

These results demonstrate that teas and hops also impact ADH activity in an tyrosinase-dependent manner. It is interesting to note that Teas 3 and 4 completed inhibited ADH with the inclusion of tyrosinase, but did not produce any effect without the oxidation catalysis. Teas 1 and 2, on the other hand, were similar to PP60 in that they inhibited ADH without tyrosinase, and the addition of tyrosinase only marginally enhanced their effects. Though the observation that individual catechol molecules can inhibit ADH may seem rather obscure to most, the ability of antioxidant compounds within commercially available products to do the same is directly relevant and of striking interest to the everyday consumer.

In sum, these ADH kinetic experiments (regarding the reverse reaction of ethanol to acetaldehyde) indicate that o-quinones are able to inhibit ADH activity, measured by the production of NADH. These effects were repeatedly observed in individual catechol compounds,

a mixture of compounds (PP60), and commercially available consumer products known to contain antioxidants.

Forward reaction kinetics

The results from the reverse reaction kinetic studies strongly suggest that o-quinones inhibit ADH activity, putatively via structural modifications. In order to corroborate these results, it is of interest to also test the enzyme kinetics in the forward or favorable reaction. In the case of ADH, this involves the reduction of acetaldehyde to ethanol, thus consuming rather than producing NADH. If the enzyme is indeed being modified by the catechol molecules, then its activity should be affected for both reaction directions, not just the reverse.

Catechol

As a preliminary test of this hypothesis, catechol was added to samples of ADH and the forward reactions kinetic procedure (as described in the methods section) was followed. Very high concentrations of catechol were used initially to obtain results.

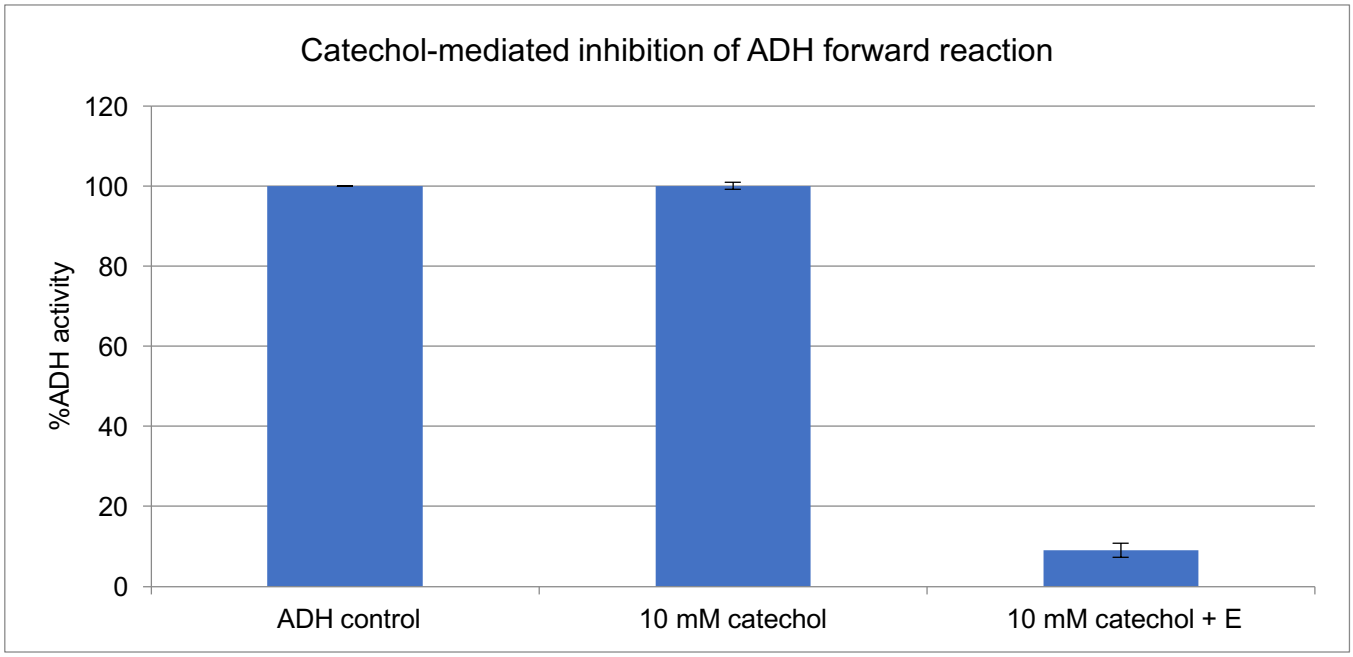

Figure 25: Samples above combined ADH and catechol. "E" indicates the addition of tyrosinase to the sample. Shown above are the averages across two trials.

This preliminary experiment clearly demonstrated the ability of catechol to inhibit ADH in the forward reaction, consistent with the results obtained in the reverse reaction experiments. From here, other catechol molecules of interest – HCA, CA, and the PP60 mixture - were also studied in the forward reaction to further corroborate previous results. HCA and CA were selected because, when oxidized, they completely inhibited ADH activity in the reverse reaction. PP60 has clear relevance to everyday life as a major component of green tea, and also demonstrated inhibitory abilities.

Hydrocaffeic acid, caffeic acid, and PP60

HCA and CA were tested at lower concentrations than catechol to match the reverse reaction, and to see if they can impact ADH activity at lower concentrations. Like catechol, both HCA and CA completely inhibited ADH at 10mM concentrations. However, in the micromolar concentration range (50-100μM), the inhibitory effects were not nearly as pronounced as they had been in the reverse reaction. Previously, ADH samples treated with tyrosinase and HCA or CA showed a 100% decrease in activity compared to the control, even at 50μM catechol. In the forward reaction, however, samples treated with HCA yielded only a 2% and 8% decrease in activity at 50μM and 100μM, respectively. Similarly, samples treated with CA showed only a 3% decrease in activity at 100μM, and no decrease at 50μM. Those treated with PP60 showed a 7% decrease in activity at 1mg/mL, and 11% at 2mg/mL.

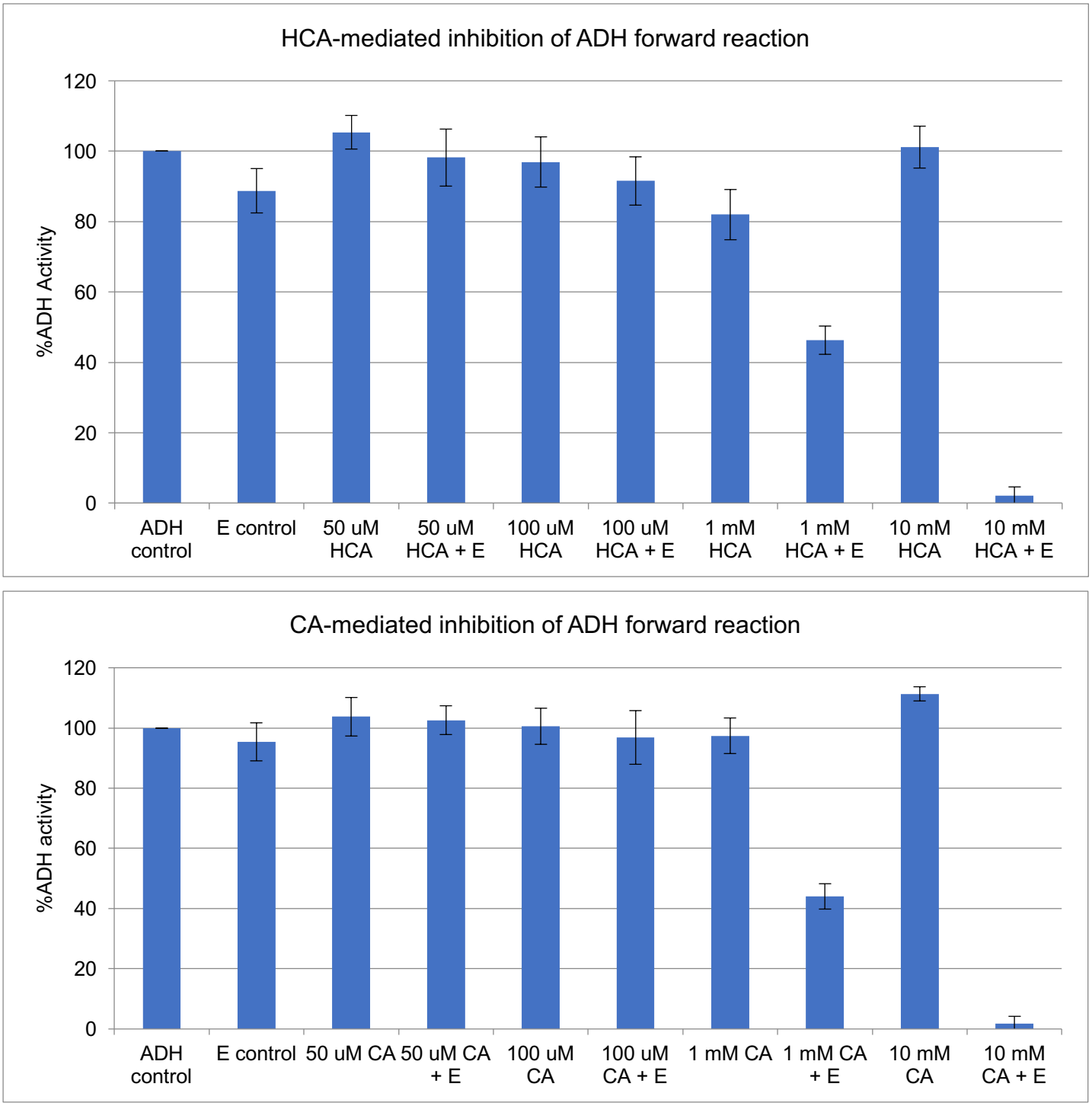

Figure 26: Samples above combined ADH and varying concentrations of HCA and CA. Shown above are the averages across eleven trials for each molecule.

PP60 was also tested at the same concentrations observed in the reverse reaction. Again, small amounts of inhibition were observed, but not nearly to the same extent as before.

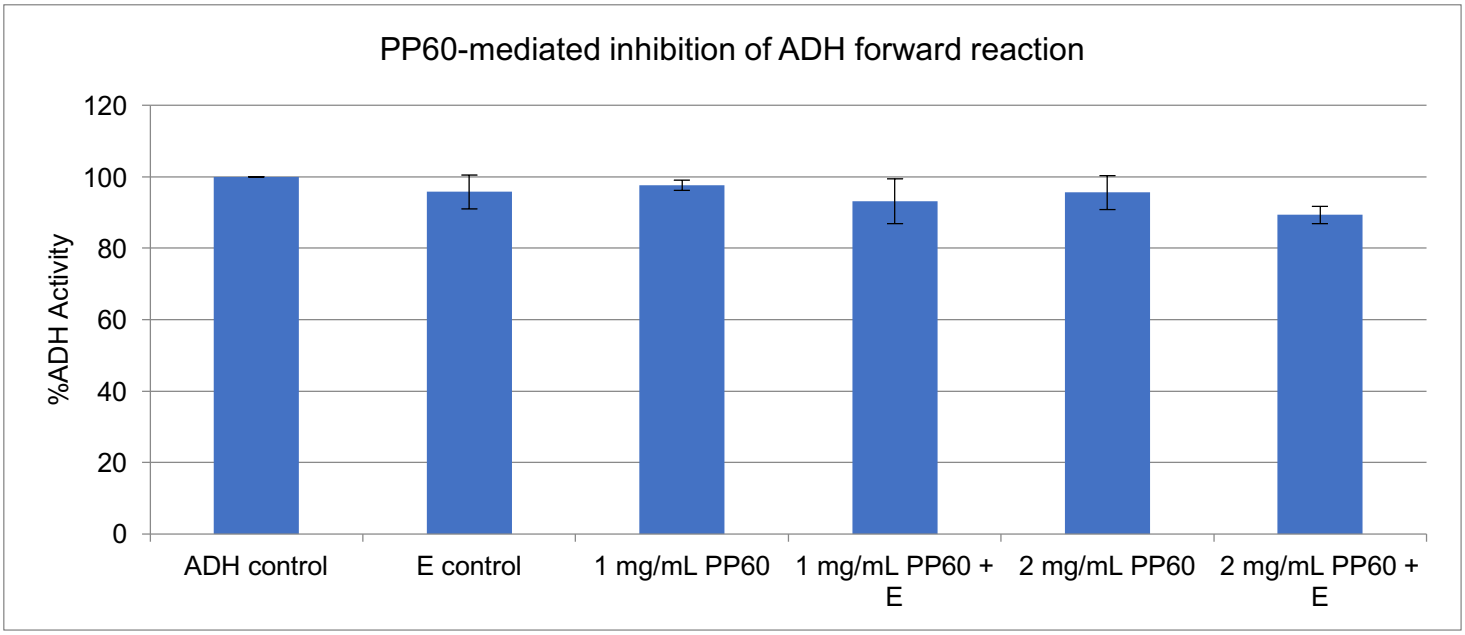

Figure 27: Samples above combined ADH and density-based amounts of PP60. Shown above are the averages across six trials. Note, again, the minimal amounts of inhibition.

We propose a few theories to explain this difference. Biochemically, though it seems intuitive that the ADH protein is performing the exact same function both for the forward and reverse reactions, it is effectively not. In the favorable reaction, ADH binds acetaldehyde and reduces it to ethanol using NADH. In the reverse reaction, it binds ethanol. Acetaldehyde and ethanol, though similar, are structurally different molecules that likely bind to ADH differently. Thus, the quinone molecules, if they are modifying the ADH, may be affecting cysteines in regions of the enzyme that are involved in ethanol binding than acetaldehyde, thus producing more dramatic effects in the reverse reaction.

As another possible explanation, the reverse reaction experiments were performed in the summer of 2017, while the forward reaction was not tested until fall of 2018. Due to this time difference, two different preparations of tyrosinase were used to catalyze catechol oxidation, and the concentration of these two samples was not standardized. The preparation used in in the

forward reaction experiments was not as concentrated as the first preparation was, and thus not as active. Therefore, it is likely that the same extent of inhibition was not observed in the forward reaction because the catechol molecules were not oxidized to the same extent. The proposed method of catechol modification of ADH (i.e. the Michael addition) requires that the catechol be oxidized. Thus, lesser extent of oxidation implies less ADH modification which in turn implies less inhibition. Despite these concentration-related differences, the results nonetheless suggest that catechol molecules are able to inhibit ADH in the forward reaction, thereby solidifying the results found in the reverse reaction.

Detecting the inhibition of ADH in living yeast cells activity using MTT/PMS absorbance assay

Catechol molecules were consistently observed to inhibit isolated ADH activity. However, this finding has no "real-world" relevance if the catechol molecules are not able to enter the yeast cell and modify the enzyme. Therefore, we created yeast samples treated with catechol molecules to determine if they are able to modify ADH within yeast cells and if so, to what extent. As per the MTT/PMS kinetics assay described in the methods section, ADH activity was determined by the final concentration of ethanol in the yeast sample supernatant. Because catechol molecules were shown to inhibit isolated ADH, we hypothesized that ADH in yeast cells would also be inhibited, thus producing less ethanol. In addition to final ethanol output, the time course of ethanol production over several days was also studied. This was to determine if the catechol compounds also impact rate of ethanol production.

Using the MTT/PMS assay, ethanol concentration was determined for each yeast sample, and averaged across molecules (i.e. the three samples treated with CA were averaged as if they were three separate trials). Ethanol output was calculated from the final absorbance read and

using it in Beer's law as the "A" value (NADH absorbance) to solve for "c", or the ethanol concentration (refer back to the methodology section for details). (Note that the absorbance of formazan, the blue molecule formed in the reduction of MTT, is what is actually being measured by the plate reader. However, recall from the methods section that NADH is produced in the oxidation of ethanol to acetaldehyde, and that the electrons are shuttled through a chain to reduce MTT in a 1:1 ratio with NADH reduction. Thus, formazan absorbance is an indirect measure of NADH absorbance.) Theoretically, the absorbance curves should level off at a certain point, and the average value of this plateau is what *should* be used to calculate concentration of ethanol in the original sample. However, the absorbance curves in this series of experiments rarely plateaued, even after three hours of reaction in the plate reader. As such, the ethanol concentration was calculated using only the individual final data point in each curve. The standard deviation across the three trials (or samples) was also calculated. (Figure 27).

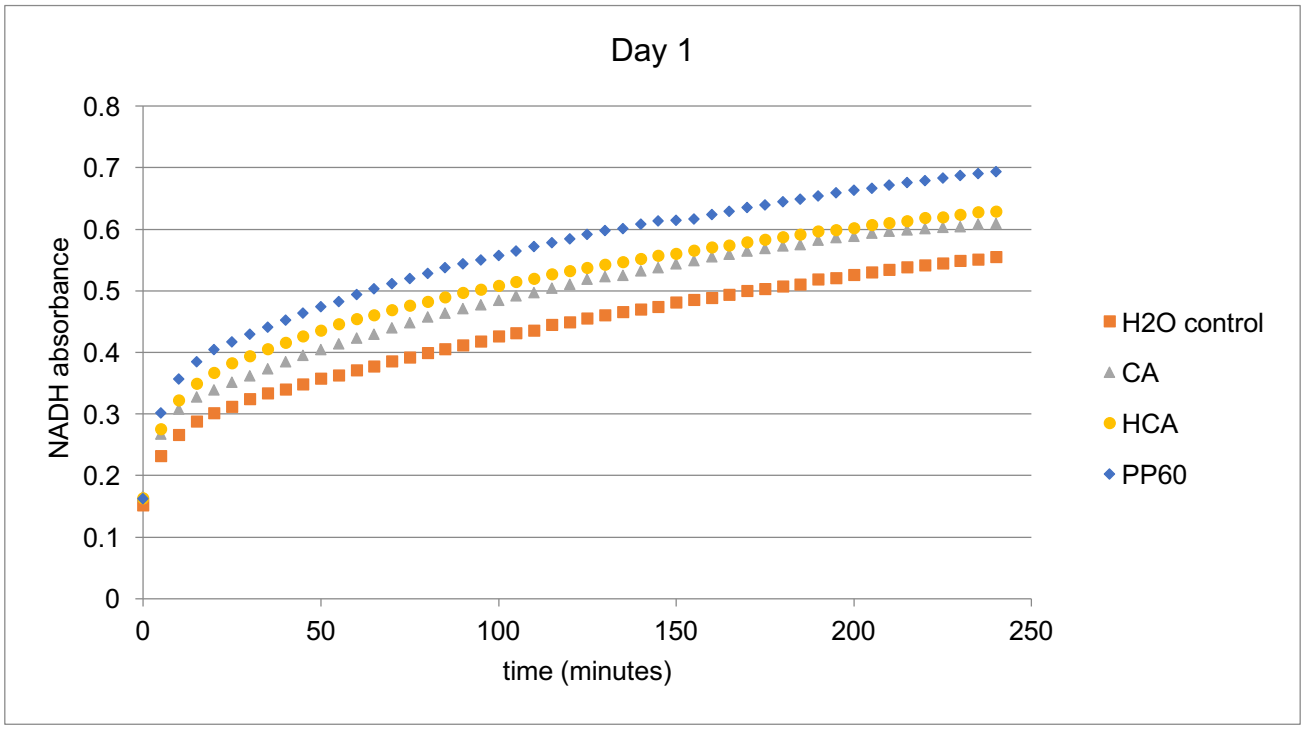

Figure 27: An example of the absorbance curves measured for different treatment groups on day 1 of a four-day experiment. Each treatment group contained 3 samples, so each data point shown is the average of absorbance of these three "trials". The standard deviation across samples was also calculated (and displayed in a table). Curves that are higher up on the y-axis have greater NADH absorbance and thus represent samples with a higher [EtOH]. These curves failed to plateau, thus only the final data point of each was used to calculate [EtOH] of the initial sample.

Instead of showing the full absorbance curves for each treatment group on each day, we show only the ethanol concentration calculated using the final data point for each group on each day to easily compare across days. This shows not only the change in ethanol concentration in individual treatment groups across days, but more importantly, allows for easy comparison across samples. That is, the stratification of data points on each day shows how similar or different the ethanol concentrations were for each treatment group, thus facilitating the easy determination of how the different molecules affected ethanol output over the course of several days.

A

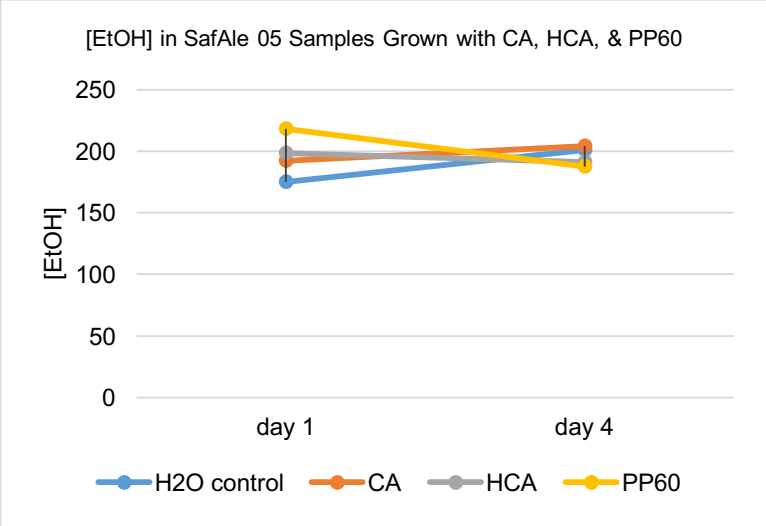

No statistically significant differences reported between samples on either day

B

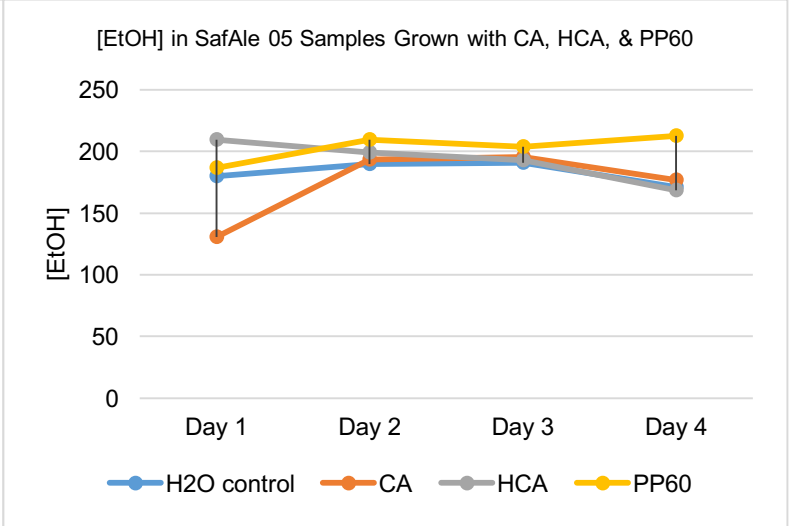

Day 1: CA is significantly less than H_2O ($p = 0.0485$), HCA ($p = 0.0062$), and PP60 ($p = 0.0398$)
Day 4: PP60 is significantly greater than H_2O ($p = 0.0081$), CA ($p = 0.0163$), and HCA ($p = 0.0061$)

C

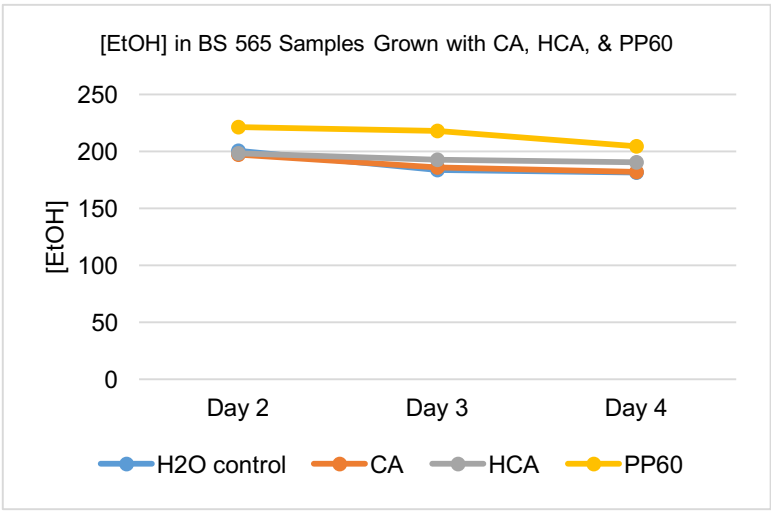

Day 1: PP60 is significantly greater than H_2O ($p = 0.0355$), CA ($p = 0.0159$), and HCA ($p = 0.0189$)
Day 2: PP60 is significantly greater than H_2O ($p = 0.0030$), CA ($p = 0.0044$), and HCA ($p = 0.0490$)
Day 3: PP60 is significantly greater than H_2O ($p = 0.045$) and CA ($p = 0.048$)

D

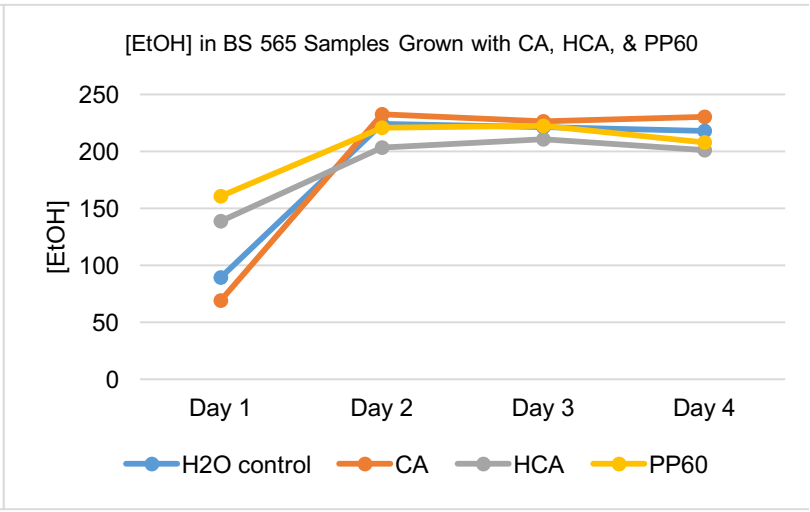

Day 1: H_2O is significantly different greater than CA ($p = 0.0357$) and significantly less than HCA ($p = 0.0001$) and PP60 ($p = 0.0000$)
CA is significantly less than HCA ($p = 0.0000$) and PP60 ($p = 0.0000$)
HCA is significantly less than PP60 ($p = 0.0242$)
Day 4: CA is significantly greater than HCA ($p = 0.0426$)

E

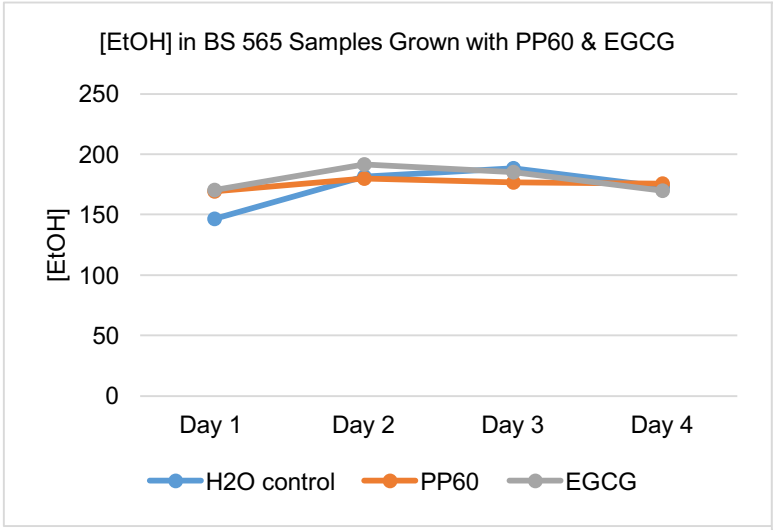

Day 1: H_2O is significantly less than PP60 ($p = 0.0029$) and EGCG ($p = 0.0024$)

F

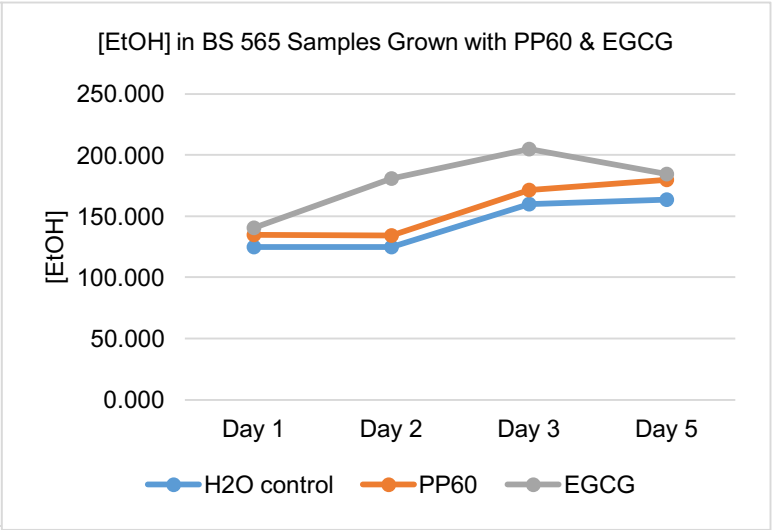

Day 1: H_2O is significantly less than EGCG ($p = 0.0204$)
Day 2: EGCG is significantly greater than H_2O ($p = 0.0002$) and PP60 ($p = 0.0009$)
Day 3: EGCG is significantly greater than H_2O ($p = 0.0011$) and PP60 ($p = 0.0055$)

G

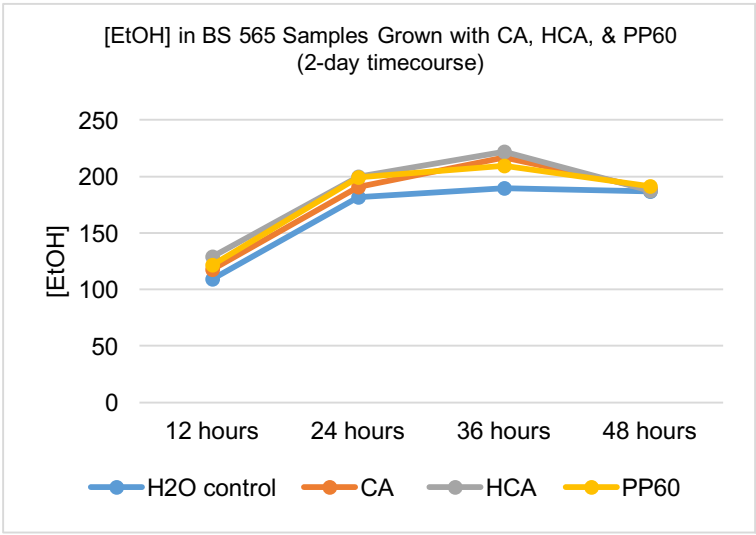

Day 1: H_2O is significantly less than HCA ($p = 0.0077$)
Day 3: H_2O is significantly less than CA ($p = 0.0200$) and HCA ($p = 0.0074$)

H

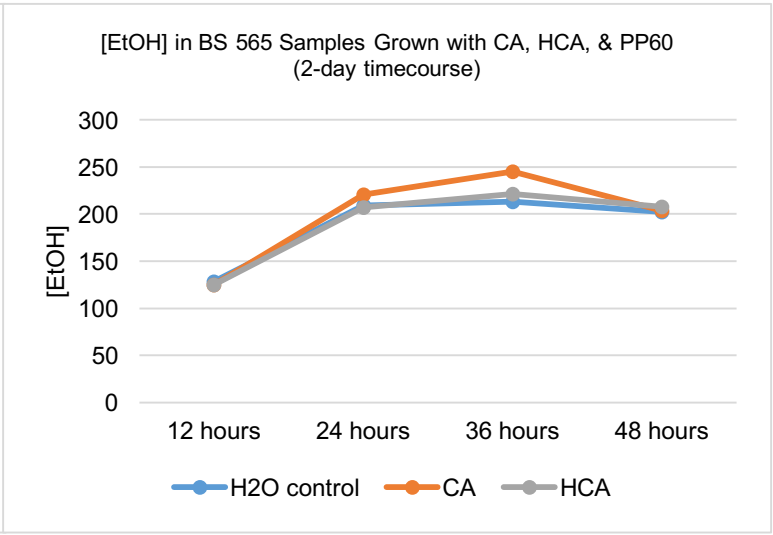

No statistically significant differences reported between samples on at any time point

Figure 29: Pictured are the results from each experiment done, in which living yeast cells were treated with a catechol molecule and induced to produce ethanol. Each chart shows the [EtOH] produced by each yeast sample (averaged across three trials) at each time point in the experiment. Listed below are the p-values for statistically significant differences in [EtOH] across samples.

A first glance at this data does not reveal any strikingly similar patterns. Neither, I would argue, does a more prolonged glance. To make this report, a classic one-way ANOVA test of statistical significance was used to determine if the amount of ethanol produced in each treatment group was significantly different than the amount produced in the H_2O control group (or from any of the other treatment groups) on any given day. A p-value of less than .05 was used to delineate significance. These values are listed underneath each results graph in Figure 28.

From analysis of these values, a few patterns do seem to stand out. In general, the concentration of ethanol among samples seems to be very spread out on Day 1, and this difference tends to disappear by Day 2. This pattern held consistently in the first six experiments (Figure 28 A-F), thus, for the last two we measured ethanol content produced only in the first two days (Figure 28 G & H). However, these last two charts fail to show any interesting difference, only confirms that there is a lower ethanol concentration across all samples at the

early time points, as could be reasonably expected. Furthermore, ethanol concentration tends to decrease by Day 4 across all samples. We propose that this occurs because the yeast have depleted their carbon source and are no longer able to produce ethanol, but rather begin to consume it by undergoing the reverse reaction.

In the cases where significant differences were recorded, two general trends seem to stand out – PP60 samples often had a greater [EtOH] than the other samples, while the H_2O control often had a lower concentration. To address the first observation made in experiments A-D, we created yeast samples treated with PP60 and EGCG, a major constituent of PP60, to see if EGCG produced similar effects on ethanol output. In experiment E, PP60 and EGCG both yielded a significantly higher concentration of ethanol than the water control at the 12-hour mark, and this difference had disappeared after 24 hours. This suggests that PP60 (and EGCG) may indeed increase initial rate of ethanol production, generating a difference which disappears with time. However, the second run through of this experiment (Figure 28 F) does not corroborate these results, and instead shows EGCG inducing the production of a significantly greater amount of ethanol across days. Perhaps PP60 does indeed somehow result in the production of more ethanol at an expedited rate, but this result was not repeated consistently enough to make any definite conclusions on the matter.

On the other hand, the second observation – that is, H_2O control samples producing generally less ethanol than the treatment groups – seemed to hold true across all experiments. Whether the difference was significant or not, the blue bar representing [EtOH] in control samples appears consistently at the bottom of the heap. This was unexpected. The results from the kinetic assays clearly indicated that catechol molecules inhibit the activity of isolated ADH. If ADH activity were also inhibited in yeast cells, the yeast would produce less ethanol, not more

as was observed. We speculate that the catechol molecules are still modifying ADH, but because a yeast cell is a more living system, there are more factors involved.

At 1.85mM in sample, the catechol molecules are likely modifying more than just ADH, as cells are filled with other proteins, lipids, and nucleic acids. These other components may also affect ethanol output. Furthermore, if ADH is indeed being inhibited, the yeast cell may upregulate gene and protein expression of glycolytic enzymes, thus potentially overcompensating and producing more ethanol than the control. Additionally, yeast use a carbon source to undergo glycolysis and produce ethanol in anaerobic conditions. We speculate that because catechols are themselves carbon sources, the yeast may be consuming these molecules as fuel as well. Investigation into these hypotheses would require yeast lysis and a comprehensive study of the other cell components being affected, as described below in the "Additional studies" section.

So what do the results of these experiments ultimately tell us? In short, there is no clear, one-line takeaway as we had with the enzyme kinetic studies of isolated ADH. Living systems are complicated, and there are many other factors at play when it comes to protein modification, gene expression, and ethanol production. It seems as though treating yeast cells with catechol molecules may somehow induce them to (counterintuitively) produce *more* ethanol, but the experiments described above are insufficient to definitively make this claim.

Detecting protein modification using native gel electrophoresis

As described in the methods section, agarose native gel electrophoresis allows for the indirect observation of protein conformational change indicated by band position on the gel, without denaturing the protein so that it maintains activity. The purpose of this procedure was to

supplement results obtained using the enzyme activity assays, while also investigating the possibility of catechol-induced ADH conformational change.

Samples were made by treating ADH with HCA and catechol, just as they were prepared for the activity assays.

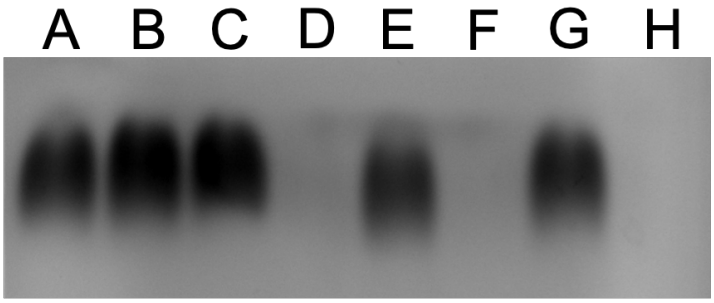

A: ADH control
B: Tyrosinase control
C: 100μM HCA
D: 100μM HCA, tyrosinase
E: 100μM catechol
F: 100μM catechol, tyrosinase
G: ADH control
H: 200μM HCA, tyrosinase

Figure 30: An example of a native gel to observe conformational and activity changes in ADH treated with oxidized catechol.

As evidenced by the example provided, there was no indication of conformational change in the catechol-treated enzyme samples. This is unlike another enzyme tested by the lab, lactate dehydrogenase (LDH), which demonstrated clear changes in band position of the treatment groups versus the control. Thus, further experiments were proposed to more closely examine the possibility of cysteine modification by oxidized catechol (see Additional studies section).

The gel does, however, clearly indicate changes in ADH activity when treated with oxidized catechol. Darker bands indicate more ADH activity. Columns D, F, and H, which contained ADH samples treated with oxidized catechols, had no activity. ADH samples treated

with catechol molecules that were not catalyzed to oxidize maintained activity, as did the assay controls. These results thus corroborate the findings reported in the enzyme kinetic assays.

Additional studies

The enzyme kinetic and gel electrophoresis experiments suggest ADH modification by o-quinones. These results are supplemented by IAF labeling studies completed in the lab by Dr. Landino. 5-Iodoacetamidofluorescein (5-IAF) is a fluorescein derivative that contains an iodoacetamido group for labeling cysteines. Reduced cysteines react with IAF to form a fluorescent protein product. If cysteines are oxidized or modified by catechols, labeling with IAF will decrease. This can be observed by SDS-PAGE or by spotting the reaction on nitrocellulose paper. The membrane is washed to remove excess reagent and small molecules, while the protein remains bound to it via hydrophobic interactions. A decrease in fluorescein labeled suggests that cysteines are modified by catechols and thus unable to react with IAF.

A redox stain can also be used to confirm that cysteines have been modified by catechols. Protein samples are prepared in the same manner as with the enzyme kinetic assays – with ADH, catechols, and tyrosinase – and spotted onto nitrocellulose. Excess reagents are again washed away. NBT in glycinate is then added as a redox stain, with the formation of a purple spot indicating protein modification (this mechanism is similar to the redox stain used in the MTT/PMS assay, with NBT serving as the redox-responsive staining molecule). Dr. Landino performed both the IAF labeling procedure and redox stain procedure on ADH samples treated with catechol and tyrosinase. In the former, fluorescence decreased, and in the latter, purple spots formed (Figure 31). Both of these results suggest protein modification.

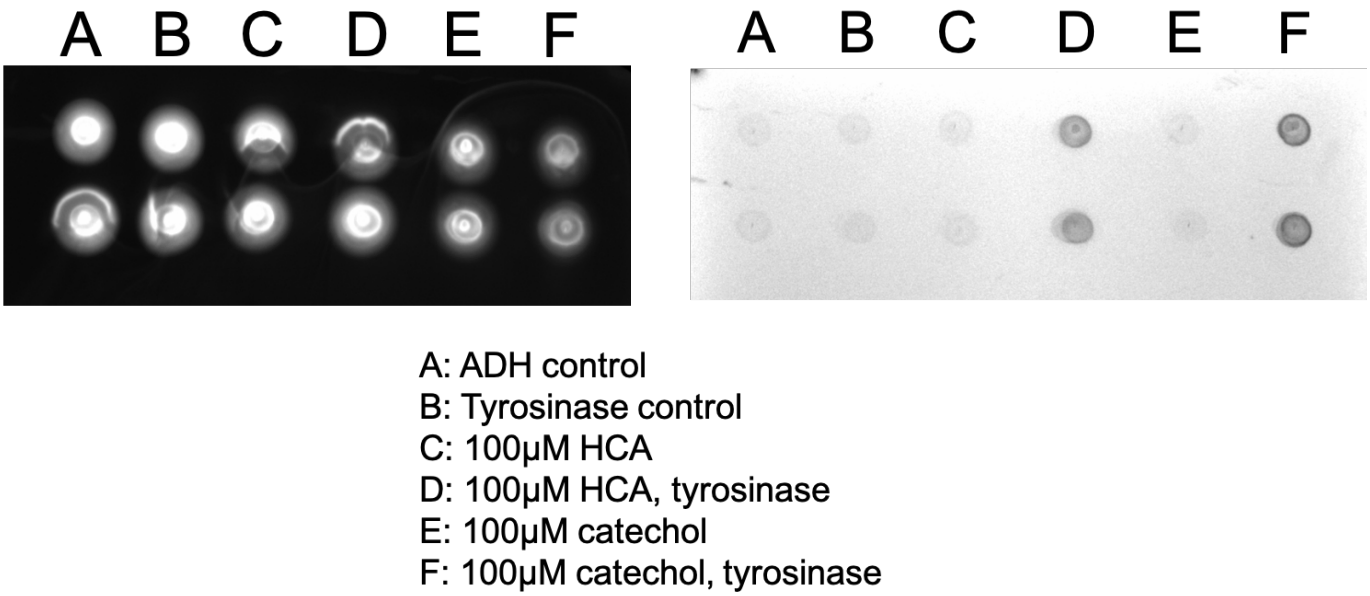

Figure 31: Left is pictured the results of the IAF labeling experiment, with a decrease in fluorescence in column F indicating cysteine modification by oxidized catechol. Column D does not show the same extent of fluorescence decrease. On the right is pictured the NBT redox stain, with darker spots in the o-quinone-treated ADH samples also indicating protein modification.

We propose to further investigate this protein modification using yeast lysis techniques. Dr. Landino's experiments demonstrate that that catechol molecules can modify isolated ADH; however, the question remains as to how catechol molecules affect ADH in living yeast cells. In a living cell, there are many components that could potentially be affected by the introduction of an exogenous molecule to the system and provide explanation for the inconsistencies seen in the MTT/PMS assay results. For example, the catechol molecule could somehow be inhibiting growth of the yeast cell itself, or impacting yeast gene and protein expression. Unlike isolated ADH, a living yeast cell contains countless other components and mechanisms that may also be impacted by the catechol molecule. By breaking open the yeast cell and then performing labeling procedures, we would be able to directly observe what exactly within the yeast cell is affected by the exogenous molecule. Like in isolated ADH, yeast ADH cysteines may indeed undergo a Michael addition with the oxidized catechol, in which case purple spots would appear following IAF labeling and spotting. But in addition to this, yeast lysis would also allow us to determine

whether the yeast cells are modifying gene expression to increase ADH production in the presence of catechol compounds.

CONCLUSION

The data reported suggested that ADH activity is inhibited by various oxidized catechol molecules. This result, as well as other work done in Dr. Landino's lab, strongly suggest that the oxidized catechol molecules modify key cysteine residues present in ADH, likely through a Michael addition. To maintain consistency with the native gel results, this modification may occur without changing the global conformation of the enzyme. Enzyme kinetic assays using isolated ADH *in vitro* consistently reported quinone-mediated inhibition of activity; however, *in vivo* studies using yeast cells did not yield the same outcome. We speculate that this is because yeast, as living systems, are affected by the exogenous molecules in many other ways, and that they may adapt to compensate for ADH modification by altering gene and protein expression. Currently, Dr. Landino's lab plans to investigate other changes occurring in the cell in conjunction with the introduction of a catechol molecule to the system. This will be explored using yeast cell lysis and fluorescence procedures. These methods can also allow us to determine if key ADH cysteines are indeed being structurally modified by oxidized catechols, as per our hypothesis.

In a disease context such as AD, these results indicate that antioxidants have the potential to contribute to oxidative damage as pro-oxidants. As described in the Background section, when mitochondria are damaged in disease states, the cell is rendered incapable of undergoing oxidative phosphorylation in aerobic respiration. Thus, cells need to upregulate glycolytic enzyme activity to produce more ATP. ADH is of critical importance in this anaerobic respiration process as it regenerates NAD+ to increase the rate of glycolysis, thus allowing for increased energy production. However, our results show that antioxidants, in particular

catechols, can inhibit ADH activity. This is the opposite of what is desired in a disease state, as it would disrupt the cell's ability to produce a sufficient amount of energy, and expedite its death.

Age-related diseases such as AD are not well understood, despite their prevalence. Thus, research that focuses on underlying mechanisms of cell death and ultimate brain tissue damage are of critical importance in the steps towards disease treatment and prevention. There exist many theories behind AD pathogenesis, primarily the APP and tau hypotheses, and many potential contributing factors to each of these pathways. Oxidative stress is one process that has been heavily implicated in neurodegeneration. As such, antioxidants have been receiving much attention in recent decades as molecules that can potentially protect against aging and age-related disease. Our research contributes to the growing pool of literature that suggests antioxidants may not be the miracle molecules they are portrayed as, but rather essential physiological compounds that also have likely negative effects. Furthermore, the role of glycolytic enzymes in this process is of special interest because glycolysis is essential in keeping a cell alive – when glycolysis fails, so does the cell. The intersection of oxidative stress and glycolysis is thus of particular interest in the context of disease states. Research investigating these facets of neurodegeneration starts to elucidate mechanisms underlying cell death and tissue decay, thus bringing us closer to a more comprehensive understanding of the physiology of stress and disease states.

APPENDIX

A. Catechol derivatives and additional phenolic compounds

Molecular structure	Compound name, molecular weight, and solubility	%ADH control activity with and without tyrosinase ("E")
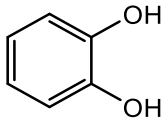	catechol MW = 110.11 430 g/L H_2O	ADH assay **Without E:** 100uM → 100 +/- 10% **With E:** 100uM → 0 +/- 2%
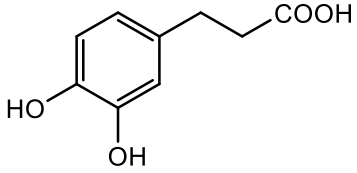	hydrocaffeic acid MW = 182.18 CAS 1078-61-1 428 mg/mL H_2O	ADH assay **Without E:** 100uM → 100 +/- 10% **With E:** 100uM → 0 +/- 2%
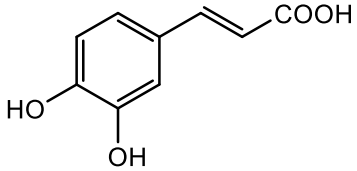	caffeic acid MW = 180.18 CAS 331-39-5 7 mg/mL DMF	ADH assay **Without E:** 100uM → 100 +/- 0.1% **With E:** 100uM → 0 +/- 0.1%
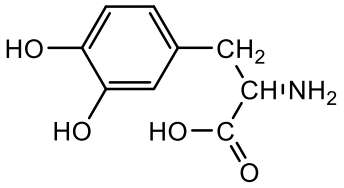	L-dopa Alfa Aesar MW = 197.19 CAS 59-92-7 5 mg/mL H_2O	ADH assay **Without E:** 100uM → 100 +/- 5% **With E:** 100uM → 30 +/- 5%

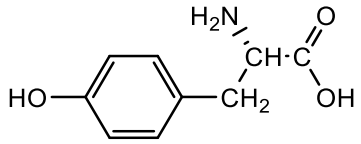	L-tyrosine Alfa Aesar MW = 181.19 .453 mg/mL H_2O	ADH assay **Without E:** 100uM → 100 +/- 10% **With E:** 100uM → 20 +/- 0.5%
catechin 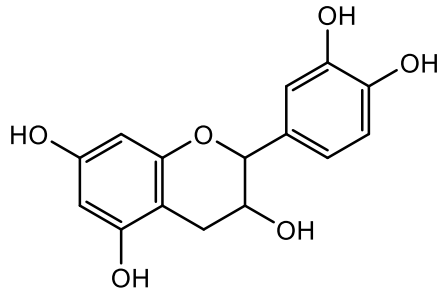	isomers exist! MW = 290.271 g/mol 100 mg/mL DMF	ADH assay **Without E:** 100uM → 100 +/- no error **With E:** 100uM → 80
T.J.'s Organic Green Tea 	1.94g/100mL	ADH assay **Without E:** 100uM → 72 +/- 2% **With E:** 100uM → 45 +/- 5%
Yogi Green Tea Kombucha 	1.94g/100mL	ADH assay **Without E:** 100uM → 85 +/- 3% **With E:** 100uM → 65 +/- 3%

Clipper Rise and Shine (Herbal) 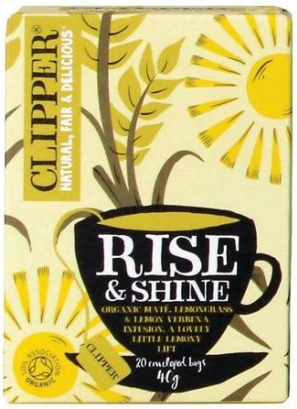	2.04g/mL	ADH assay **Without E:** 100uM → 100 +/- 7% **With E:** 100uM → 0 +/- 0.5%
Yerba Mate (Herbal) 	3.09g/100mL	ADH assay: **Without E:** undiluted extract → 100 +/- 5% **With E:** undiluted extract → 0 +/- 1%
PP60 Green Tea Extract	0.2mg/mL	ADH assay: **Without E:** 0.2 mg/mL → 70 +/- 25% **With E:** 0.2 mg/mL → 45 +/- 10%

German Hallertau HOPs (2.5% alpha) 	1.0g/50mL	ADH assay: **Without E:** undiluted extract → 100 +/- 2% **With E:** undiluted extract → 45 +/- 5%
Cascade HOPs (8.4% alpha, 7.5% beta) 	1.0g/50mL	ADH assay: **Without E:** undiluted extract → 100 +/- 15% **With E:** undiluted extract → 60 +/- 2%
Apollo Hop Pellets (15-19% alpha, 5.5-8% beta) 	1.0g/50mL	ADH assay: **Without E:** undiluted extract → 100 +/- 2% **With E:** undiluted extract → 75 +/- 2%

B. Yeast ADH structure with labeled important amino acids (PDB file 4W6Z)

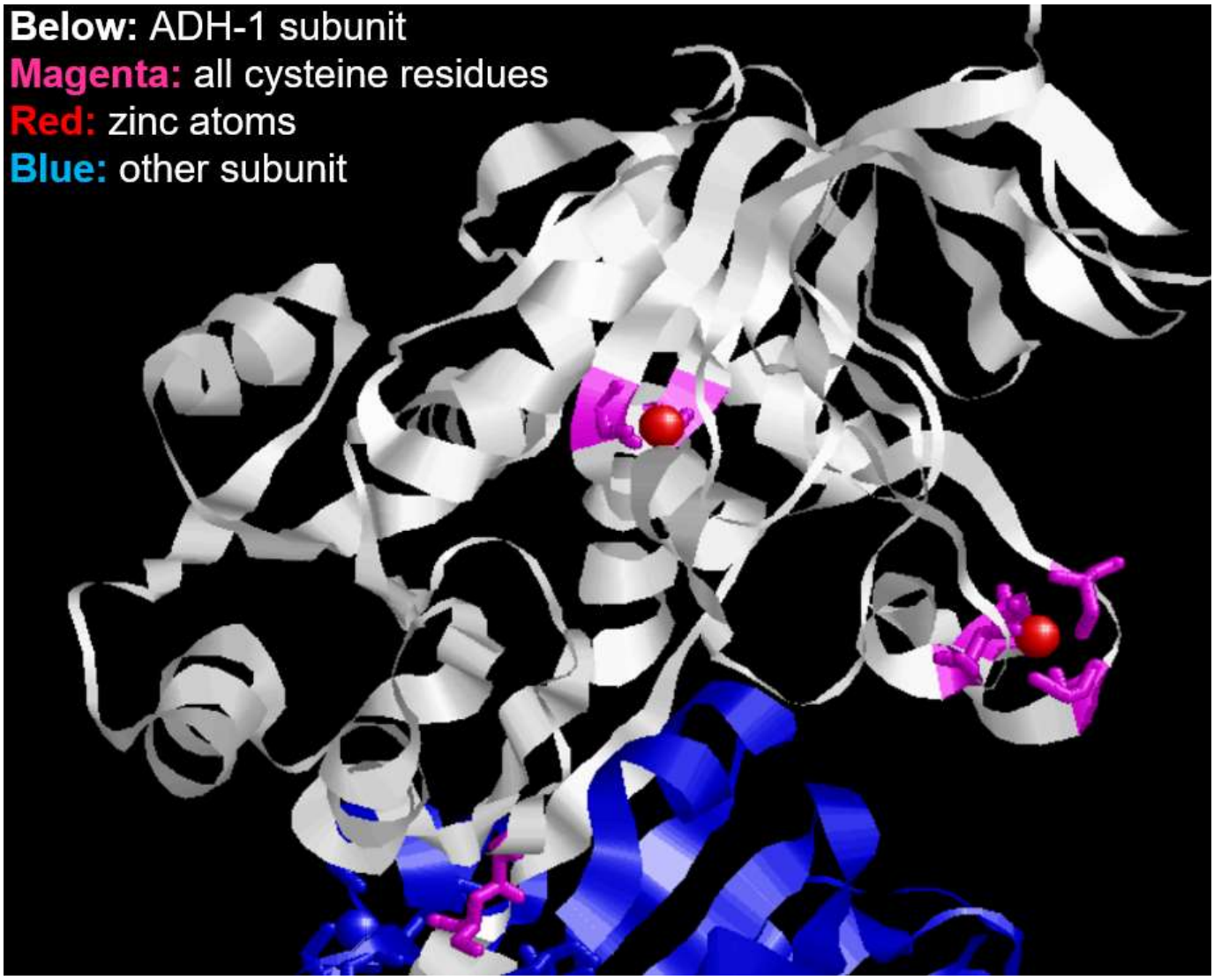

Image taken from Lydia Boike Honors Thesis Fall 2017

C. Yeast ADH single subunit amino acid sequence with cysteines highlighted (PDB 4W6Z)

IPETQ KGVIF YESHG KLEYK

DIPVP KPKAN ELLIN VKYSG

VCHTD LHAWH GDWPL PVKLP

LVGGH EGAGV VVGMG ENVKG

WKIGD YAGIK WLNGS CMACE

YCELG NESNC PHADL SGYTH

DGSFQ QYATA DAVQA AHIPQ

GTDLA QVAPI LCAGI TVYKA

LKSAN LMAGH WVAIS GAAGG

LGSLA VQYAK AMGYR VLGID

GGEGK EELFR SIGGE VFIDF

TKEKD IVGAV LKATD GGAHG

VINVS VSEAA IEAST RYVRA

NGTTV LVGMP AGAKC CSDVF

NQVVK SISIV GSYVG NRADT

REALD FFARG LVKSP IKVVG

LSTLP EIYEK MEKGQ IVGRY VVDTS

K

REFERENCES

Azhar, S. H. M., Abdulla, R., Jambo, S. A., Marbawi, H., Gansau, J. A., Faik, A. A. M., & Rodrigues, K. F. (2017). Yeast in sustainable bioethanol production: A review. *Biochemistry and Biophysics Reports, 10*, 52-61. doi: 10.1016/j.bbrep.2017.03.003

Bouayed, J., & Bohn, T. (2010). Exogenous antioxidants – Double-edged swords in cellular redox state. *Oxidative Medicine and Cellular Longevity, 3*(4), 228-237. doi: 10.4161/oxim.3.4.12858

Bolton, J. L., & Dunlap, T. (2017). Formation and biological targets of quinones: Cytotoxic versus cytoprotective effects. *Chemical Research in Toxicology, 30*, 13-37. doi: 10.1021/acs.chemrestox.6b00256

Botstein, D., Chervitz, S. A., & Cherry, J. M. (1997). Yeast as a model organism. *Science, 277*(5330), 1259-1260.

Braz, V. A., & Howard, K. J. (2009). Separation of protein oligomers by blue native gel electrophoresis. *Analytical Biochem, 388*(1), 170-172. doi:10.1016/j.ab.2009.02.019

Carocho, M., & Ferreira, I. C. F. R. (2013). A review on antioxidants, prooxidants and related controversy: Natural and synthetic compounds, screening and analysis methodologies and future perspectives. *Food and Chemical Toxicology, 51*, 15-25. doi: 10.1016/j.fct.2012.09.021

Chow, V. W., Mattson, M. P., Wong, P. C., & Gleichmann, M. (2010). An overview of APP processing enzymes and products. *Neuromolecular Medicine, 12*(1), 1-12.

Halliwell, B. (2007). Biochemistry of oxidative stress. *Biochemical Society Transactions, 35*(5), 1147-1150. doi: 10.1042/BST0351147

Hardy, J., & Selkoe, D. J. (2002). The amyloid hypothesis of Alzheimer's disease: Progress and problems on the road to therapeutics. *Science, 297*(5580), 353-356. doi: 10.1126/science.1072994

Huang, H. C., & Jiang, Z. F. (2009). Accumulated amyloid- β peptide and hyperphosphorylated tau protein: Relationship and links in Alzheimer's disease. *Journal of Alzheimer's Disease, 16*, 15-27. doi: 10.3233/JAD-2009-0960

Kametani, F., & Hasegawa, M. (2018). Reconsideration of amyloid hypothesis and tau hypothesis in Alzheimer's disease. *Frontiers in Neuroscience, 12*(25). doi: 10.3389/fnins.2018.00025

Kim, J., & Dang, C. V. (2005). Multifaceted roles of glycolytic enzymes. *TRENDS in Biochemical Sciences, 30*(3), 142-150. doi:10.1016/j.tibs.2005.01.005

Lobo, V., Patil, A., Phatak, A., Chandra, N. (2010). Free radicals, antioxidants, and functional foods: Impact on human health. *Pharmacognosy Reviews, 4*(8), 118-126. doi: 10.4103/0973-7847.70902

Lu, J. M., Lin, P. H., Yao, Q., Chen, C. (2010). Chemical and molecular mechanisms of antioxidants: experimental approaches and model systems. *Molecular Medicine, 14*(4), 840-860. doi: 10.1111/j.1582-4934.2009.00897

Raj, S. B., Ramaswamy, S., & Plapp, B. V. (2014). Yeast Alcohol Dehydrogenase Structure and Catalysis. *Biochemistry, 53*, 5791-5803. doi: 10.1021/bi5006442

Revett, T. J., Baker, G. B., Jhamandas, J., & Kar, S. (2013). Glutamate system, amyloid β peptides and tau protein: functional interrelationships and relevance to Alzheimer disease pathology. *Journal of Psychiatry & Neuroscience, 38*(1), 6-23. doi: 10.1503/jpn.110190

Sawada, G. A., Williams, L. R., Lutzke, B. S., & Raub, T. J. (1999). Novel, highly lipophilic antioxidants readily diffuse across the blood-brain barrier and access intracellular sites. *The Journal of Pharmacology and Experimental Therapeutics, 288*, 1327-1333.

Smith, M. A., Rottkamp, C. A., Nunomura, A., Raina, A. K., & Perry, G. (2000). Oxidative stress in Alzheimer's disease. *Biochimica et Biophysica Acta, 1502*(1), 139-144. doi: 10.1016/S0925-4439(00)00040-5

Zhou, Y., Shi, J., Chu, D., Hu, W., Guan, Z., Gong, C. X., … Liu, F. (2018). Relevance of phosphorylation and truncation of tau to the etiopathogenesis of Alzheimer's disease. *Frontiers in Aging Neuroscience, 10*(27). doi: 10.3389/fnagi.2018.00027

Thank you to the Charles Center and William & Mary and the English-Stonehouse Fellowship for aiding in the funding of this project.

Special thank you to Dr. Lisa Landino for providing invaluable mentorship and guidance.